

Chern-Simons-Modified-RPA-Eliashberg Theory of the $\nu = \frac{1}{2} + \frac{1}{2}$ Quantum Hall Bilayer

Tevž Lotrič and Steven H. Simon

Rudolf Peierls Centre for Theoretical Physics, Parks Road, Oxford, OX1 3PU, UK

The $\nu = \frac{1}{2} + \frac{1}{2}$ quantum Hall bilayer has been previously modeled using Chern-Simons-RPA-Eliashberg (CSRPAE) theory to describe pairing between the two layers. However, these approaches are troubled by a number of divergences and ambiguities. By using a “modified” RPA approximation to account for mass renormalization, we can work in a limit where the cyclotron frequency is taken to infinity, effectively projecting to a single Landau level. This, surprisingly, controls the important divergences and removes ambiguities found in prior attempts at CSRPAE. Examining BCS pairing of composite fermions we find that the angular momentum channel $l = +1$ dominates for all distances d between layers and at all frequency scales. Examining BCS pairing of composite fermion electrons in one layer with composite fermion *holes* in the opposite layer, we find the $l = 0$ pairing channel dominates for all d and all frequencies. The strength of the pairing in these two different descriptions of the same phase of matter is found to be almost identical. This agrees well with our understanding that these are two different but dual descriptions of the same phase of matter.

Quantum Hall bilayers have been a subject of intense investigation since the first experiments on these systems almost thirty years ago (see Refs. [1–3] for reviews). Conceptually, these are simple systems: a pair of parallel two-dimensional electron gases separated by a distance d placed in a magnetic field at low temperature. Nonetheless, they show a vast variety of fascinating phenomena. Perhaps the problem that has attracted the most interest in this field has been the case of the balanced bilayer with Landau level filling fraction $\nu = \frac{1}{2} + \frac{1}{2}$. In the limit of small distance d between the layers (compared to the magnetic length ℓ_B) the system forms an exciton condensate[1] (alternately called a quantum Hall ferromagnet[4] or the Halperin “111” state[5]). In this state one can think of each electron in one layer being bound to a correlation hole in the opposite layer, hence forming an exciton. In contrast, in the limit of large d/ℓ_B the system can be considered as two independent $\nu = \frac{1}{2}$ quantum Hall systems, which are known to be composite fermion Fermi liquids[6–8].

The composite fermion Fermi liquid may be described either with a Jain wavefunction approach[8], by attaching two Jastrow factors to the position of each electron, or in a Chern-Simons field theory[6, 7, 9] approach, where a singular gauge transformation is made to attach two infinitely thin flux tubes to each fermion. One can also consider the state as being described by a Fermi liquid of composite fermion *holes*. That is, one thinks of the holes in a filled Landau level as being the fundamental degrees of freedom, and attaches flux quanta (or Jastrow factors) to these holes. For clarity if we mean composite fermion holes we will abbreviate them as CH, whereas when we mean conventional composite fermions, where flux quanta, or Jastrow factors, are attached to the original electron coordinate, we will abbreviate this as CE. The distinction between the CE and CH Fermi liquids, two states that are related to each other by particle-hole conjugation within a single Landau level, is discussed in some detail by Refs. [10, 11]. The CE and CH approaches to the half-filled Landau level are supplemented by the Dirac composite fermion approach[12], which explicitly

preserves particle-hole symmetry of the half-filled Landau level. Although appearing quite different, it is now generally believed that the long wavelength universal physics of the CE Fermi liquid, the CH Fermi liquid, and the Dirac composite Fermi liquid are equivalent (see, for example, [11, 13–15]).

Returning now to the $\nu = \frac{1}{2} + \frac{1}{2}$ bilayer, although the two limits of large and small distance d between the layers have been quite well understood for some time, the question that has occupied the community for years[1, 3, 4, 16–49] is what happens for intermediate d/ℓ_B . Only recently a clear picture has finally emerged as to the physics of this regime. Based partially on the Dirac composite fermion picture[12], Sodemann et al. proposed that the two CE Fermi liquids, when weakly interacting with each other, should BCS pair in the $l = +1$ angular momentum channel (chiral p-wave), and they further proposed that this phase of matter is continuously connected to the exciton condensate at $d = 0$. The idea of BCS pairing of CEs in such bilayers was not new[18, 35, 36, 49, 50], but it was not previously clear that the BCS paired state of CEs could be the same phase of matter as the exciton condensate.

Inspired by new experiments in bilayers built from graphene[16, 17], an alternative picture was recently constructed. In this picture one imagines condensing BCS pairs made from a CE in one layer bound to a CH of the other layer in the $l = 0$ angular momentum channel (s-wave). This then gives an apparently different picture of a paired state. What is emphasized in Ref. [16] (supplement) is that in this picture, in the limit of tightly bound pairs, projection to the lowest Landau level gives precisely the exciton condensate, or Halperin 111 state.

To test these two pictures of interlayer pairing, Wagner et al. [51] (see also Ref. [52]) constructed Jain-style[8] trial wavefunctions for BCS paired states both for $l = +1$ CE-CE pairing and for $l = 0$ CE-CH pairing. (These constructions were both based on earlier work of Möller, Simon, and Rezayi [35].) Both approaches were found to be extremely accurate for all values of d when compared with exact diagonalizations on small systems (square

overlaps $\gtrsim .97$ for system sizes of 6+6 electrons on a sphere where the symmetry-reduced Hilbert space is 252 dimensional), and the two approaches were essentially indistinguishable in how well they performed. We conclude that both approaches are describing the same physics — although the mapping between the two approaches is nontrivial.

To try to access the thermodynamic limit, and in order to gain more physical intuition, one can attempt to address the pairing between the two layers analytically. Very early in the history of the field, Bonesteel, MacDonald and Nayak [18] described the CEs in each layer using the Halperin-Lee-Read (HLR) Chern-Simons field theory[6]. The bosonic “glue” that pairs the fermions together between the two layers is the Chern-Simons RPA screened Coulomb interaction. Ref. [18] then used Eliashberg theory to evaluate the pairing instability, the result of which we call Chern-Simons-RPA-Eliashberg theory (abbreviated CSRPAE). Although such calculations are plagued with divergences, these authors were nonetheless able to argue that the system would be unstable to pairing at any finite d , although at the level of this calculation all angular momentum channels of pairing are degenerate.

A more detailed version of this CSRPAE calculation was attempted much later by Isobe and Fu[53] (other versions were attempted by Refs. [49, 54]). To control infra-red divergences, Isobe and Fu introduced a wavevector cutoff q_c which is taken to be a very small fraction of the Fermi momentum. There are two coupling constants that are calculated in this Eliashberg theory: $\lambda_Z(\omega_m)$, the prefactor of the non-anomalous electron self-energy, which in this calculation diverges as $1/q_c$ at any (fermion) Matsubara frequency ω_m and is independent of the pairing channel, and $\lambda_\phi^{(l)}(\omega_m)$, the prefactor of the anomalous self-energy, which in this calculation diverges as $\log(q_c)$ at any nonzero Matsubara frequency and depends on the pairing channel l . (There are additional, but integrable, divergences as ω_m goes to zero, which do not need to be regularized). Despite these divergences, it was found that the *difference* between the coupling constants $\lambda_\phi^{(l)}(\omega_m)$ in different pairing channels l is non-divergent, so that the arbitrary cutoff need not be implemented when comparing different channels to each other, thus suggesting that the arbitrary cutoff may not be problematic. In particular, the claim of Isobe and Fu was that the pairing angular momentum channel $l = +1$ is always favored, i.e., $\lambda_\phi^{(l)}(\omega_m)$ is always most negative for $l = +1$. This pairing channel agreed with earlier trial wavefunction work of Möller, Simon, Rezayi[35] as well as with the more recent predictions of Sodemann et al. [39]. However, upon repeating this calculation we found that while $l = +1$ often minimizes $\lambda_\phi^{(l)}$, it can sometimes (depending on ω_m and d) be minimized instead with $l \neq +1$ (see examples of this in our supplementary material[55], section I), making it hard to draw conclusions confidently as to which pairing channel is actually favored.

Recently the Isobe-Fu calculation[53] was generalized by Rüegg, Chaudhary, and Slager[56] to consider the alternative picture of CEs in one layer and CHs in the other layer. Again, within CSRPAE theory, the leading divergent terms are independent of pairing channel and one relies on a cutoff to regularize the calculation, although differences in pairing strength are non-divergent allows comparison between different pairings. The calculation found that the $l = 0$ pairing channel for CE-CH pairing is favored, in agreement with the trial wavefunctions of Ref. [51]. In addition, the authors claimed that the CE-CH pairing is stronger than the CE-CE pairing. This latter point is a somewhat curious result when compared to the trial wavefunction results of Wagner et al[51] where both trial wavefunctions seem equivalently good. In fact, the comparison made by Rüegg, Chaudhary, and Slager[56] between CE-CE pairing and CE-CH pairing is questionable because the two approaches have different divergent terms, so comparison of the coupling strengths depends on how these divergences are regularized (see Supplementary material[55], sections II and IV). While it is always the case that CE-CH pairing is favored compared to CE-CE pairing, i.e., $\lambda_\phi^{(l=0),\text{CE-CH}}(\omega_m) < \lambda_\phi^{(l=+1),\text{CE-CE}}(\omega_m)$, depending on the cutoff and ω_m this inequality may either be greatly unequal or may be very close to an equality.

The above mentioned Chern-Simons Eliashberg calculations[18, 53, 56] are excellent starting points for further analytic work which we shall pursue here. These prior calculations, however, have a number of clear shortcomings: (1) As mentioned above, the CSRPAE calculations with CE-CE pairing are somewhat ambiguous in which pairing channel is actually favored (supplementary material[55], section I). (2) The introduction of an arbitrary infra-red cutoff is somewhat unsatisfying and gives room to doubt that the results are reliable. (3) The fact that CE-CE and CE-CH pairing have different divergences makes it impossible to compare these two calculations in a cutoff-independent way (supplementary material [55] section IV). (4) The CSRPAE calculations are based on RPA evaluation of a propagator and RPA is known to have a number of problems — in particular RPA does not correctly put the low energy physics on the interaction scale and the high energy physics on the cyclotron scale[6, 57]. (5) In making comparison of the CSRPAE approach with the successful trial wavefunctions of Wagner et al.[51] one may also worry that the wavefunctions are strictly in the lowest Landau level, whereas Chern-Simons RPA theory is not. As detailed in Supplementary material[55] section VI, this is particularly concerning in the case of CH calculations where one cannot even use “hole” coordinates as the fundamental degrees of freedom unless the system has a finite Hilbert space dimension, such as when the system is projected to a single Landau level.

The purpose of this paper is to repair the many problems of these previous works and for the first time obtain unambiguous results. This letter will report our main

findings with the calculational details relegated to the Supplement[55]. Surprisingly, a single new physical ingredient added to the prior calculations can, to a large extent, address *all* of the above listed shortcomings. In this paper we extend the CSRPAE calculations to use a so-called *modified* RPA (MRPA) approach developed by Simon and Halperin[57], rather than the pure RPA. This scheme, based on Landau Fermi liquid theory, puts the low energy physics on the interaction scale while pushing the cyclotron mode up to the correct frequency so that Kohn's theorem and the f-sum rule are properly satisfied. Setting the cyclotron energy $\omega_c = eB/m_b$ to infinity (i.e., taking the limit of the electron bare band mass m_b going to zero) then should remove any physics of this high energy scale from the problem. While this is not strictly equivalent to lowest Landau level projection, presumably much of the same physics is included.

We now briefly describe the calculation. More details are given in the Supplement[55]. The MRPA scheme[9, 57] accounts for mass renormalization via Landau Fermi theory. The polarization bubble for noninteracting fermions in zero effective field is calculated with an effective mass m^* which is set by the interaction scale. To preserve sum rules (stemming from Galilean invariance) we must include a Landau Fermi liquid interaction which amounts to an additional current-current interaction term $A \mathbf{j} \cdot \mathbf{j}$ with $A = (m_b - m^*)/(ne^2)$ with n the electron density and e the electron charge and \mathbf{j} the current density. This current-current interaction term is then treated in RPA along with the Chern-Simons gauge interaction and the Coulomb interaction. The remainder of the Chern-Simons Eliashberg calculation follows that of Refs. [53, 56] and is detailed in Supplementary material[55] section III. Using MRPA rather than RPA in CSRPAE theory we thus abbreviate as CSMRPAE. If we set $m^* = m_b$ in CSMRPAE we recover the CSRPAE results of Refs. [53, 56].

We now consider CSMRPAE in the limit of m_b going to zero. This limit is meant to represent projection to a single Landau level, although as mentioned in Supplementary material section VI, once one makes any sort of mean field approximation, some of the detailed structure of the lowest Landau level is lost, such as its particle-hole symmetry. Remarkably, in this limit we find that the divergences in coupling constants $\lambda_Z(\omega_m)$ and $\lambda_\phi^{(l)}(\omega_m)$ vanish proportional to m_b^n with $n \geq 1$ for any value of ω_m such that $0 < \omega_m < \mathcal{O}(\omega_c)$ (see Supplementary material[55] section IV, V) for both CE-CE pairing and for CE-CH pairing. By taking the $m_b \rightarrow 0$ limit, we push ω_c to infinity, removing all divergences at any finite frequency, and thus remove the need for an ad-hoc q_c cutoff.

In this limit, we find that for CE-CE pairing $l = +1$ is now unambiguously the strongest pairing channel for all values of d and ω_m (see Fig. 1 and Supplementary material[55] section VII), and for CE-CH pairing $l = 0$ remains unambiguously the strongest pairing channel (see Fig. 1 Supplementary material[55] section VIII). Further, without the divergences and cutoff dependencies we can

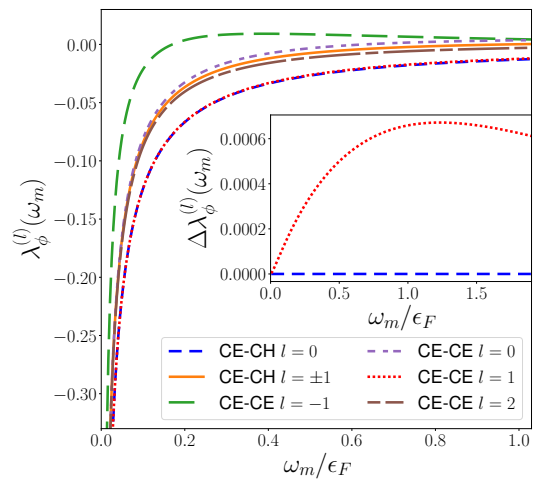


FIG. 1. The Eliashberg anomalous coupling constant $\lambda_\phi^{(l)}(\omega_m)$ calculated using CSMRPAE for interlayer spacing $d/l_B = 1$. The coupling constant is shown for different pairing channels l and for both composite-fermion-electron-composite-fermion-electron pairing (CE-CE) and for composite-fermion-electron-composite-fermion-hole pairing (CE-CH). We see that CE-CH pairing with $l = 0$ and CE-CE pairing with $l = 1$ are most attractive (most negative) and are very nearly equal to each other (the two lowest curves almost precisely overlap). The inset shows a blow up of the difference between the two lowest curves ($l = 0$, CE-CH pairing and $l = 0$ CE-CE pairing). The difference is a factor of order 100 smaller than the difference to other pairing channels. Other values of d/l_B , and larger range of ω_m are shown in the Supplement[55] section VII.

now meaningfully compare CE-CE $l = +1$ pairing with CE-CH $l = 0$ pairing. To very high precision (roughly one percent level) we find that CE-CE pairing and CE-CH pairing are equivalently strong (see Fig. 1, inset). This equivalence is rather surprising given that two very different integrals need to give almost precisely the same result. We show further (Supplementary material section VIII D) what small modification of our MRPA approximation would make them exactly equal.

We note in passing that, as pointed out in Ref. [51] (see supplement therein) both CE-CE and CE-CH pairing are equally able to remain paired in the presence of density imbalance between the layers, so long as the total filling remains $\nu_T = 1$, in agreement with experiment[58, 59]. We reiterate this argument in Supplementary material[55] section IX. Imbalance will be studied in more depth in a forthcoming work.

To conclude, we believe our approach of looking at the $m_b \rightarrow 0$ limit of CSMRPAE has satisfactorily tamed the divergences and ambiguities of CSRPAE theory which have been problematic for several decades. Our results are: for CE-CE pairing the $l = +1$ pairing channel is unambiguously the strongest, and for CE-CH pairing the $l = 0$ pairing channel is unambiguously the strongest. To very high precision we also find that these two cases pair with the same strength in agreement with the results of prior trial wavefunction calculations[51]. This is rather

satisfying since we believe that the two types of pairing are simply different descriptions of the same physics. In fact, it is perhaps a bit surprising that our two approximate approaches are so closely equivalent given that we have not enforced any sort of symmetry between the two. One might think that this near equivalence is a result of particle-hole symmetry (which itself has been broken by the Chern-Simons calculational approach even in the $m_b \rightarrow 0$ limit). However, even given a perfect particle-hole symmetry, it is not obvious that binding CEs to CEs

should be precisely equivalent to binding CEs to CHs. This should be interpreted as a nontrivial duality which is surprisingly accurately respected by the CSMRPAE approach.

Acknowledgements: TL was supported by the Rudolph Peierls Centre for Theoretical Physics UROP summer internship. SHS is funded by EPSRC grant EP/S020527/1. Statement of compliance with EPSRC policy framework on research data: This publication is theoretical work that does not require supporting research data.

-
- [1] J. Eisenstein, Exciton condensation in bilayer quantum hall systems, *Annual Review of Condensed Matter Physics* **5**, 159 (2014).
- [2] S. Das Sarma and A. Pinczuk, eds., *Perspectives in Quantum Hall Effects: Novel Quantum Liquids in Low-Dimensional Semiconductor Structures* (Wiley, 1996).
- [3] J. P. Eisenstein and A. H. MacDonald, Bose–einstein condensation of excitons in bilayer electron systems, *Nature* **432**, 691 (2004).
- [4] K. Moon, H. Mori, K. Yang, S. M. Girvin, A. H. MacDonald, L. Zheng, D. Yoshioka, and S.-C. Zhang, Spontaneous interlayer coherence in double-layer quantum hall systems: Charged vortices and kosterlitz-thouless phase transitions, *Phys. Rev. B* **51**, 5138 (1995).
- [5] B. I. Halperin, Theory of the quantized Hall conductance, *Helv. Phys. Acta* **56**, 75 (1983).
- [6] B. I. Halperin, P. A. Lee, and N. Read, Theory of the half-filled landau level, *Phys. Rev. B* **47**, 7312 (1993).
- [7] O. Heinonen, ed., *Composite Fermions: A Unified View of the Quantum Hall Regime* (World Scientific, 1998).
- [8] J. K. Jain, *Composite Fermions* (Cambridge University Press, 2007).
- [9] S. H. Simon, The chern-simons fermi liquid description of fractional quantum hall state, chapter in ref. [7], arXiv [10.48550/arXiv.cond-mat/9812186](https://arxiv.org/abs/10.48550/arXiv.cond-mat/9812186) (1998).
- [10] M. Barkeshli, M. Mulligan, and M. P. A. Fisher, Particle-hole symmetry and the composite fermi liquid, *Phys. Rev. B* **92**, 165125 (2015).
- [11] S. D. Geraedts, J. Wang, E. H. Rezayi, and F. D. M. Haldane, Berry phase and model wave function in the half-filled landau level, *Phys. Rev. Lett.* **121**, 147202 (2018).
- [12] D. T. Son, Is the composite fermion a dirac particle?, *Phys. Rev. X* **5**, 031027 (2015).
- [13] A. K. C. Cheung, S. Raghu, and M. Mulligan, Weiss oscillations and particle-hole symmetry at the half-filled landau level, *Phys. Rev. B* **95**, 235424 (2017).
- [14] C. Wang, N. R. Cooper, B. I. Halperin, and A. Stern, Particle-hole symmetry in the fermion-chern-simons and dirac descriptions of a half-filled landau level, *Phys. Rev. X* **7**, 031029 (2017).
- [15] S. D. Geraedts, M. P. Zaletel, R. S. K. Mong, M. A. Metlitski, A. Vishwanath, and O. I. Motrunich, The half-filled landau level: The case for dirac composite fermions, *Science* **352**, 197 (2016).
- [16] X. Liu, J. I. A. Li, K. Watanabe, T. Taniguchi, J. Hone, B. I. Halperin, P. Kim, and C. R. Dean, Crossover between strongly coupled and weakly coupled exciton superfluids, *Science* **375**, 205 (2022), <https://www.science.org/doi/pdf/10.1126/science.abg1110>.
- [17] X. Liu, Z. Hao, K. Watanabe, T. Taniguchi, B. I. Halperin, and P. Kim, Interlayer fractional quantum hall effect in a coupled graphene double layer, *Nature Physics* **15**, 893 (2019).
- [18] N. E. Bonesteel, I. A. MacDonald, and C. Nayak, Gauge fields and pairing in double-layer composite fermion metals, *Phys. Rev. Lett.* **77**, 3009 (1996).
- [19] H. Isobe and L. Fu, Interlayer pairing symmetry of composite fermions in quantum hall bilayers, *Phys. Rev. Lett.* **118**, 166401 (2017).
- [20] T. Morinari, Composite-fermion pairing in bilayer quantum hall systems, *Phys. Rev. B* **59**, 7320 (1999).
- [21] Z. F. Ezawa and G. Tsitsishvili, Quantum hall ferromagnets, *Reports on Progress in Physics* **72**, 086502 (2009).
- [22] B. Lian and S.-C. Zhang, Wave function and emergent $su(2)$ symmetry in the $\nu_T = 1$ quantum hall bilayer, *Phys. Rev. Lett.* **120**, 077601 (2018).
- [23] Y. N. Joglekar and A. H. MacDonald, Microscopic functional integral theory of quantum fluctuations in double-layer quantum hall ferromagnets, *Phys. Rev. B* **64**, 155315 (2001).
- [24] Y. N. Joglekar and A. H. MacDonald, Is there a dc josephson effect in bilayer quantum hall systems?, *Phys. Rev. Lett.* **87**, 196802 (2001).
- [25] Y. N. Joglekar and A. H. MacDonald, Bias-voltage-induced phase transition in bilayer quantum hall ferromagnets, *Phys. Rev. B* **65**, 235319 (2002).
- [26] A. H. MacDonald, P. M. Platzman, and G. S. Boebinger, Collapse of integer hall gaps in a double-quantum-well system, *Phys. Rev. Lett.* **65**, 775 (1990).
- [27] H. A. Fertig, Energy spectrum of a layered system in a strong magnetic field, *Phys. Rev. B* **40**, 1087 (1989).
- [28] R. Côté, L. Brey, and A. H. MacDonald, Broken-symmetry ground states for the two-dimensional electron gas in a double-quantum-well system, *Phys. Rev. B* **46**, 10239 (1992).
- [29] Z. Zhu, L. Fu, and D. N. Sheng, Numerical study of quantum hall bilayers at total filling $\nu_T = 1$: A new phase at intermediate layer distances, *Phys. Rev. Lett.* **119**, 177601 (2017).
- [30] K. Nomura and D. Yoshioka, Evolution of $\nu = 1$ bilayer quantum hall ferromagnet, *Phys. Rev. B* **66**, 153310 (2002).
- [31] J. Schliemann, S. M. Girvin, and A. H. MacDonald, Strong correlation to weak correlation phase transition in bilayer quantum hall systems, *Phys. Rev. Lett.* **86**, 1849 (2001).
- [32] N. Shibata and D. Yoshioka, Ground state of $\nu = 1$ bilayer quantum hall systems, *Journal of the Physical Society of*

- Japan **75**, 043712 (2006).
- [33] K. Park, Spontaneous pseudospin spiral order in bilayer quantum hall systems, *Phys. Rev. B* **69**, 045319 (2004).
- [34] K. Park and S. Das Sarma, Coherent tunneling in exciton condensates of bilayer quantum hall systems, *Phys. Rev. B* **74**, 035338 (2006).
- [35] G. Möller, S. H. Simon, and E. H. Rezayi, Trial wave functions for $\nu = \frac{1}{2} + \frac{1}{2}$ quantum hall bilayers, *Phys. Rev. B* **79**, 125106 (2009).
- [36] G. Möller, S. H. Simon, and E. H. Rezayi, Paired composite fermion phase of quantum hall bilayers at $\nu = \frac{1}{2} + \frac{1}{2}$, *Phys. Rev. Lett.* **101**, 176803 (2008).
- [37] S. H. Simon, E. H. Rezayi, and M. V. Milovanovic, Coexistence of composite bosons and composite fermions in $\nu = \frac{1}{2} + \frac{1}{2}$ quantum hall bilayers, *Phys. Rev. Lett.* **91**, 046803 (2003).
- [38] Y.-H. Zhang and I. Kimchi, Paired exciton condensate and topological charge-4e composite fermion pairing in half-filled quantum Hall bilayers, arXiv e-prints, arXiv:1810.02809 (2018), [arXiv:1810.02809](https://arxiv.org/abs/1810.02809) [cond-mat.str-el].
- [39] I. Sodemann, I. Kimchi, C. Wang, and T. Senthil, Composite fermion duality for half-filled multicomponent Landau levels, *Phys. Rev. B* **95**, 085135 (2017).
- [40] M. V. Milovanović, E. Dobardžić, and Z. Papić, Meron deconfinement in the quantum hall bilayer at intermediate distances, *Phys. Rev. B* **92**, 195311 (2015).
- [41] J. Ye, Fractional charges and quantum phase transitions in imbalanced bilayer quantum hall systems, *Phys. Rev. Lett.* **97**, 236803 (2006).
- [42] J. Ye and L. Jiang, Quantum phase transitions in bilayer quantum hall systems at a total filling factor $\nu_T = 1$, *Phys. Rev. Lett.* **98**, 236802 (2007).
- [43] J. Alicea, O. I. Motrunich, G. Refael, and M. P. A. Fisher, Interlayer coherent composite fermi liquid phase in quantum hall bilayers, *Phys. Rev. Lett.* **103**, 256403 (2009).
- [44] R. Cipri, *Gauge Fields and Composite Fermions in Bilayer Quantum Hall Systems*, Ph.D. thesis, Florida State University (2014).
- [45] R. Cipri and N. E. Bonesteel, Gauge fluctuations and interlayer coherence in bilayer composite fermion metals, *Phys. Rev. B* **89**, 085109 (2014).
- [46] Z. Papić, *Fractional quantum Hall effect in multicomponent systems*, Ph.D. thesis, Université Paris Sud-Paris XI (2010).
- [47] R. L. Doretto, C. Morais Smith, and A. O. Caldeira, Finite-momentum condensate of magnetic excitons in a bilayer quantum hall system, *Phys. Rev. B* **86**, 035326 (2012).
- [48] R. L. Doretto, A. O. Caldeira, and C. M. Smith, Bosonization approach for bilayer quantum hall systems at $\nu_T = 1$, *Phys. Rev. Lett.* **97**, 186401 (2006).
- [49] Z. Wang, I. Mandal, S. B. Chung, and S. Chakravarty, Pairing in half-filled Landau level, *Annals of Physics* **351**, 727 (2014).
- [50] N. E. Bonesteel, Compressible phase of a double-layer electron system with total Landau-level filling factor 1/2, *Phys. Rev. B* **48**, 11484 (1993).
- [51] G. Wagner, D. X. Nguyen, S. H. Simon, and B. I. Halperin, *s*-wave paired electron and hole composite fermion trial state for quantum hall bilayers with $\nu = 1$, *Phys. Rev. Lett.* **127**, 246803 (2021).
- [52] Q. Hu, T. Neupert, and G. Wagner, Single-parameter variational wavefunctions for quantum hall bilayers, arXiv:2303.12825.
- [53] H. Isobe and L. Fu, Interlayer Pairing Symmetry of Composite Fermions in Quantum Hall Bilayers, *Phys. Rev. Lett.* **118**, 166401 (2017).
- [54] L. Mendoza, *Pairing and Pair Breaking in Bilayer Composite Fermion Metals*, Ph.D. thesis, Florida State University (2020).
- [55] T. Lotrič and S. H. Simon, Chern-Simons Eliashberg theory of the $\nu = \frac{1}{2} + \frac{1}{2}$ quantum hall bilayer: importance of mass renormalization, Supplementary material.
- [56] L. Rüegg, G. Chaudhary, and R.-J. Slager, Pairing of Composite-Electrons and Composite-Holes in $\nu_T = 1$ Quantum Hall Bilayers, arXiv [10.48550/arXiv.2303.10212](https://arxiv.org/abs/10.48550/arXiv.2303.10212) (2023).
- [57] S. H. Simon and B. I. Halperin, Finite-wave-vector electromagnetic response of fractional quantized hall states, *Phys. Rev. B* **48**, 17368 (1993).
- [58] A. R. Champagne, A. D. K. Finck, J. P. Eisenstein, L. N. Pfeiffer, and K. W. West, Charge imbalance and bilayer two-dimensional electron systems at $\nu_T = 1$, *Phys. Rev. B* **78**, 205310 (2008).
- [59] I. B. Spielman, M. Kellogg, J. P. Eisenstein, L. N. Pfeiffer, and K. W. West, Onset of interlayer phase coherence in a bilayer two-dimensional electron system: Effect of layer density imbalance, *Phys. Rev. B* **70**, 081303 (2004).
- [60] G. A. Ummaryno, Eliashberg theory, in *Emergent Phenomena in Correlated Matter* (Forschungszentrum Jülich, 2013).
- [61] A. Lopez and E. Fradkin, Fractional quantum hall effect and Chern-Simons gauge theories, *Phys. Rev. B* **44**, 5246 (1991).
- [62] S. He, S. H. Simon, and B. I. Halperin, Response function of the fractional quantized hall state on a sphere. ii. exact diagonalization, *Phys. Rev. B* **50**, 1823 (1994).
- [63] G. Möller and S. H. Simon, Composite fermions in a negative effective magnetic field: A Monte Carlo study, *Phys. Rev. B* **72**, 045344 (2005).
- [64] C. Kallin and B. I. Halperin, Excitations from a filled Landau level in the two-dimensional electron gas, *Phys. Rev. B* **30**, 5655 (1984).

Supplementary Material for:

Chern-Simons-Modified-RPA-Eliashberg Theory of the $\nu = \frac{1}{2} + \frac{1}{2}$ Quantum Hall Bilayer

Tevž Lotrič and Steven H. Simon

I. RESULTS OF ISOBE-FU CALCULATION

In this section we reproduce results of the Isobe-Fu calculation[53] which are based on RPA. While that work claimed that the $l = +1$ pairing channel is always favored, we find that their results have some ambiguity. In particular, at higher frequencies, higher values of angular momenta l can be favored with the transition occurring at lower frequency for larger d . A more detailed calculation would be required to confirm the claim of Ref. [53] that $l = +1$ is always the most stable pairing channel.

Fig. 2a reproduces the results of Isobe-Fu [53] Figure 2(a), extending the range of ω_m up to $2\epsilon_F$. We show the anomalous self-energy coupling constants $\lambda_\phi^{(l)}(\omega_m)$ as a function of ω_m when $d = 1/k_F = l_B$ (the definition of this coupling is given in Ref. [53], but also in Eq. 38 below). Negative coupling constant corresponds to an attractive interaction.

In Fig. 2b we show coupling constants as a function of ω_m for $d = 3/k_F = 3l_B$ instead. In both cases, we see the $l = 1$ channel is the strongest at low frequency, before eventually being replaced by $l = 2$ at high enough frequency. In fact at very high ω_m , the channels with larger $|l|$ are preferred (although at high frequency $\lambda_\phi^{(l)}(\omega_m) > 0$, while a negative value is required for attraction).

While it seems plausible that $l = +1$ is the dominant pairing channel since it is the most attractive at low frequency, without further calculation, strictly speaking, it is ambiguous since higher l 's can be more attractive at finite frequency.

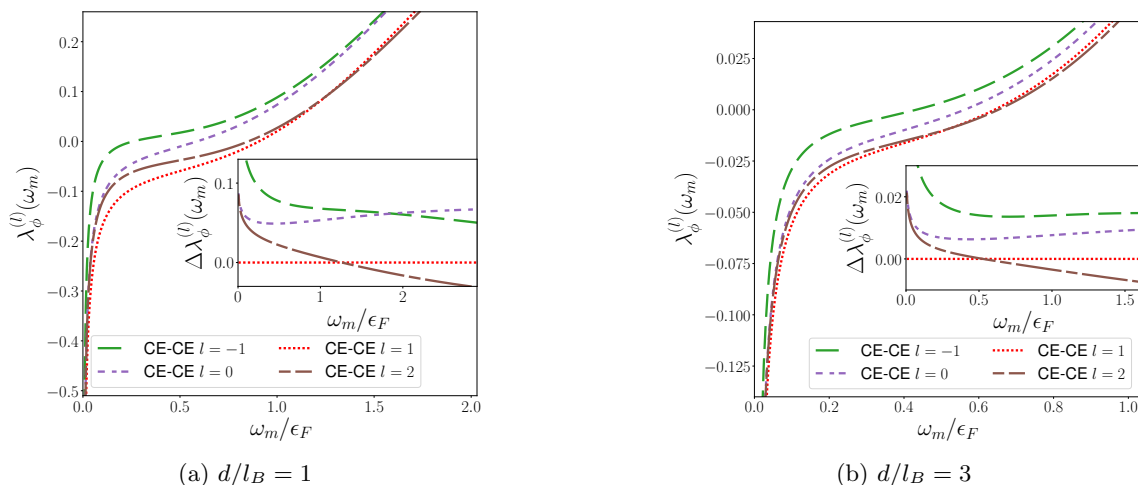


FIG. 2. The results for $\lambda_\phi^{(l)}(\omega_m)$ from the Isobe-Fu [53] calculation recreated, showing ambiguity in the favoured channel at high frequency. The insets show the behaviour relative to the possibly-favoured $l = +1$ channel. To regularise divergences, we used a cutoff $q_c = 10^{-5} \cdot k_F$ in the Eliashberg integrals, Eq. 38. This matches the cutoff used by Isobe-Fu.

II. THE AMBIGUITY OF COMPARING CE-CE TO CE-CH WITHIN RPA

While the introduction of an arbitrary cutoff does not change the ordering of the different CE-CE pairing channels in strength when comparing them to each other, that is no longer the case when comparing CE-CE channels to CE-CH channels. In this section, we present numerical results showing that the comparison between CE-CE and CE-CH channels (as done by [56]) significantly depends on the cutoff q_c chosen. Later, in Section IV, we analytically show that the divergent term for CE-CH coupling is exactly opposite to that for CE-CE coupling. Focusing on Fig. 3, we can clearly see the lines crossing at different frequencies in Fig. 3a with $q_c = 10^{-3} \cdot k_F$, compared to Fig. 3b with $q_c = 10^{-7} \cdot k_F$: for example, at $\omega_m = 0.7\epsilon_F$, Fig. 3a suggests that CE-CE $l = 1$ should be favoured over CE-CH

$l = \pm 1$, while Fig. 3b suggests CE-CH $l = \pm 1$ is the stronger one out of the two. Furthermore, the difference between CE-CH $l = 0$ and CE-CE $l = 1$ significantly depends on the cutoff chosen: the insets show that the difference more than doubles when going from $q_c = 10^{-3} \cdot k_F$ to $q_c = 10^{-7} \cdot k_F$. This makes it hard to interpret the results of [56], where proper care was not taken to handle this divergence. We note that within the $m_b = 0$ MRPA, the low- q divergence is removed, so the results in Fig. 1 do not rely on any cutoff. As such they are unambiguous in showing which coupling channels are favoured at what frequency and the gaps between channels do not depend on the cutoff chosen.

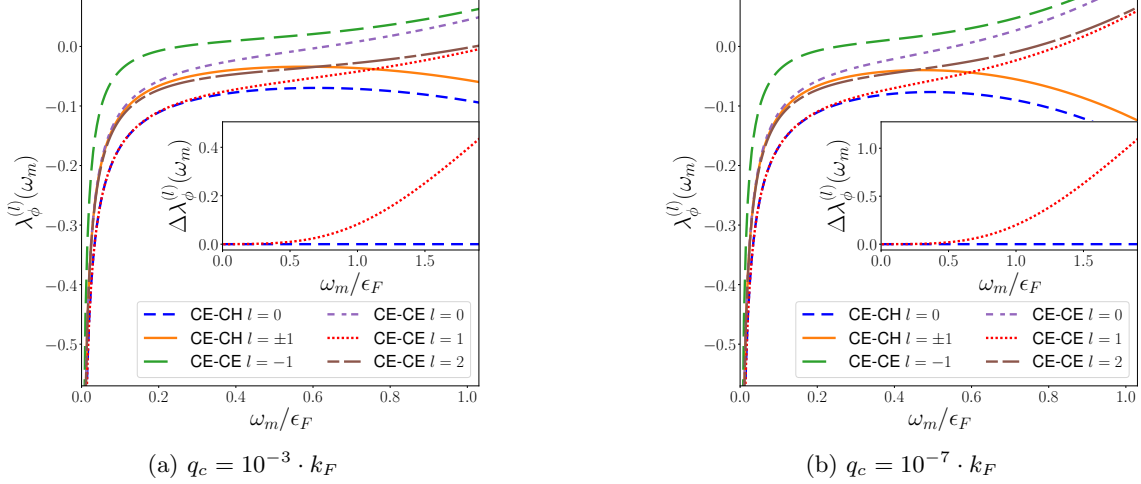


FIG. 3. The different dependence of CE-CE pairing channels on the cutoff relative to the CE-CH channels: at certain frequencies, changing the cutoff can change the ordering of the different channels in pairing strength. The insets show the difference between the two most promising candidates: CE-CE $l = 1$ and CE-CH $l = 0$. At any fixed ω_m , the difference between the two varies significantly as the cutoff is changed.

III. DETAILS OF MRPA CHERN-SIMONS ELIASHBERG THEORY

Our calculation closely follows that of Isobe and Fu's paper [53] and that of Rüegg, Chaudhary, and Slager [56]. In this section, we briefly explain their computation, and show how it is modified to include the MRPA.

A. RPA and MRPA propagators

We start with the standard HLR Lagrangian [6], adapting it to two layers, adding a Coulomb interaction between the layers, and introducing a charge parameter, c_s , in each layer. A layer of CE's has $c_s = 1$ and a layer of CH's has $c_s = -1$. In Euclidian form, the action is [53, 56]

$$\begin{aligned}
 S = \sum_{s \in \{1,2\}} \int d\tau d^2\mathbf{x} \left[\psi_s^\dagger (\partial_\tau + ia_0^{(s)} - c_s iA_0 - \mu_s) \psi_s + \frac{1}{2m^*} \psi_s^\dagger \left(i\nabla + \mathbf{a}^{(s)} - c_s \mathbf{A} \right)^2 \psi_s - \frac{c_s i}{4\pi} a_0^{(s)} \hat{z} \cdot (\nabla \times \mathbf{a}^{(s)}) \right] \\
 + \frac{1}{2} \sum_{s,s' \in \{1,2\}} c_s c_{s'} \int d\tau d^2\mathbf{x} d^2\mathbf{y} \delta\rho_s(\mathbf{y}, \tau) V_{ss'}(|\mathbf{y} - \mathbf{x}|) \delta\rho_{s'}(\mathbf{x}, \tau).
 \end{aligned} \tag{1}$$

Here, $V_{ss'}(r) = \frac{e^2}{\epsilon\sqrt{r^2 + (1 - \delta_{ss'})d^2}}$ is the Coulomb interaction between the composite fermions (CFs), and $\delta\rho_s(\mathbf{x}, \tau) = \psi_s^\dagger(\mathbf{x}, \tau)\psi_s(\mathbf{x}, \tau) - n_e$ is the CF density fluctuation.

We start with the mean-field solution and account for fluctuations within the RPA. First notice that $a_0^{(s)}$ only appears linearly in S , so it acts as a Lagrange multiplier, enforcing

$$\psi_s^\dagger \psi_s = \frac{c_s}{4\pi} \hat{z} \cdot (\nabla \times \mathbf{a}^{(s)}) \tag{2}$$

The system is at half-filling, so $B = \nabla \times \mathbf{A} = B = \frac{2\pi}{\nu} n_e = 4\pi n_e$. The mean field may thus be identified as $\delta\rho_s = 0$ and $\mathbf{a}^{(s)} = c_s \mathbf{A}$. To expand around the mean field, we let $\mathbf{a}^{(s)} = c_s \mathbf{A} + \tilde{\mathbf{a}}^{(s)}$ and use Eq. 2 on the interaction term in Eq. 1. This gives us

$$S = \sum_{s \in \{1,2\}} \int d\tau d^2 \mathbf{x} \left[\psi_s^\dagger (\partial_\tau + i\tilde{a}_0^{(s)} - \mu_s) \psi_s - i\tilde{a}_0^{(s)} n_e + \frac{1}{2m^*} \psi_s^\dagger \left(i\nabla + \tilde{\mathbf{a}}^{(s)} \right)^2 \psi_s - \frac{c_s i}{4\pi} \tilde{a}_0^{(s)} \hat{z} \cdot \left(\nabla \times \tilde{\mathbf{a}}^{(s)} \right) \right] \\ + \frac{1}{2} \frac{1}{(4\pi)^2} \sum_{s,s' \in \{1,2\}} \int d\tau d^2 \mathbf{x} d^2 \mathbf{y} \hat{z} \cdot \left[\nabla \times \tilde{\mathbf{a}}^{(s)}(\mathbf{y}, \tau) \right] V_{ss'}(|\mathbf{y} - \mathbf{x}|) \hat{z} \cdot \left[\nabla \times \tilde{\mathbf{a}}^{(s')}(\mathbf{y}, \tau) \right]. \quad (3)$$

We move to Fourier space, choosing to continue in the Coulomb gauge for $\tilde{\mathbf{a}}^{(s)}$, $\nabla \cdot \tilde{\mathbf{a}}^{(s)} = 0$, dropping the tilde from now on. In the Coulomb gauge, we may write $\mathbf{a}^{(s)}(\mathbf{q}, \tau) = a_1^{(s)}(\mathbf{q}, \tau)(\hat{z} \times \hat{\mathbf{q}})$. The action in Fourier space is

$$S[a_\mu, \psi_s^\dagger, \psi] = S_a[a_\mu] + S_{af}[a_\mu, \psi_s^\dagger, \psi_s] \quad (4)$$

$$S_a[a_\mu] = \frac{1}{2} \sum_{\omega_m} \int \frac{d^2 q}{(2\pi)^2} \sum_{s,s' \in \{1,2\}} \sum_{\mu,\nu \in \{0,1\}} a_\mu^{(s)}(\mathbf{q}, i\omega_m) \left[\mathcal{D}^{(0)}(q, i\omega_m) \right]_{\mu s, \nu s'}^{-1} a_\nu^{(s')}(-\mathbf{q}, -i\omega_m) \quad (5)$$

$$\left[\mathcal{D}^{(0)}(q, i\omega_m) \right]_{\mu s, \nu s'}^{-1} = \begin{pmatrix} 0 & \frac{q}{4\pi} \delta_{ss'} \\ \frac{q}{4\pi} \delta_{ss'} & -\frac{q^2 V_{ss'}(q)}{(4\pi)^2} \end{pmatrix}_{\mu\nu} \quad (6)$$

$$S_{af}[a_\mu, \psi_s^\dagger, \psi_s] = \sum_{s \in \{1,2\}} \sum_{\omega_m, \epsilon_n} \int \frac{d^2 k}{(2\pi)^2} \frac{d^2 q}{(2\pi)^2} \quad (7)$$

$$\times \psi_s^\dagger(\mathbf{q} + \mathbf{k}, i\epsilon_n + i\omega_m) \left[(2\pi)^2 \delta^{(2)}(\mathbf{q}) \delta_{\omega_m, 0} \left(-i\epsilon_n + \frac{k^2}{2m^*} - \mu_s \right) + \phi(\mathbf{q}, \mathbf{k}, i\omega_m) \right] \psi_s(\mathbf{k}, i\epsilon_n)$$

$$\phi(\mathbf{q}, \mathbf{k}, i\omega_m) = i a_0^{(s)}(\mathbf{q}, i\omega_m) - \frac{1}{m^*} [\hat{z} \cdot (\hat{\mathbf{q}} \times \mathbf{k})] a_1^{(s)}(\mathbf{q}, i\omega_m) \quad (8)$$

$$+ \frac{1}{2m^*} \sum_{\omega_p} \int \frac{d^2 p}{(2\pi)^2} a_1^{(s)}(\mathbf{p} + \mathbf{q}, i\omega_m + i\omega_p) \frac{(\mathbf{p} + \mathbf{q}) \cdot (-\mathbf{p})}{|\mathbf{p} + \mathbf{q}| |\mathbf{p}|} a_1^{(s)}(-\mathbf{p}, -i\omega_p)$$

where ω_m is a bosonic Matsubara frequency and ϵ_n is a fermionic Matsubara frequency. $V_{ss'}(q) = \frac{2\pi e^2}{\epsilon q} e^{-qd(1-\delta_{ss'})}$ is the Fourier transformed Coulomb interaction. The RPA is performed by integrating out the fermionic degrees of freedom, and proceeding to expand the result to second order in the gauge fields $a_\mu^{(s)}(\mathbf{q}, i\omega_m)$. Since the action is quadratic in the fermionic fields, the first step is simple, yielding

$$\mathcal{Z} = \int D(a_\mu) e^{-S_a[a_\mu]} \int D(\psi^\dagger, \psi) e^{-S_{af}[a_\mu, \psi^\dagger, \psi]} = \int D(a_\mu) e^{-S_a[a_\mu]} \det \left[-\hat{G}_0 + \hat{\phi} \right] = \int D(a_\mu) e^{-S_a[a_\mu] - \Delta S[a_\mu]} \quad (9)$$

$$\Delta S = -\ln \det \left[-\hat{G}_0^{-1} + \hat{\phi} \right] = -\text{tr} \ln \left[-\hat{G}_0^{-1} + \hat{\phi} \right] = -\ln \text{tr} \left[-\hat{G}_0^{-1} \right] + \text{tr} \left[\hat{G}_0 \hat{\phi} \right] + \frac{1}{2} \text{tr} \left[\hat{G}_0 \hat{\phi} \hat{G}_0 \hat{\phi} \right] + \dots \quad (10)$$

Here, \hat{G}_0 is an operator diagonal in momentum and frequency, whose diagonal elements are the fermionic propagators, $G(\mathbf{q}, i\epsilon_n) = \frac{1}{i\epsilon_n - \xi_{\mathbf{q}}}$, with $\xi_{\mathbf{q}} = \frac{q^2}{2m^*} - \mu$. The operator $\hat{\phi}$ is not diagonal in the momenta: the amplitude for a momentum transfer \mathbf{q} and energy transfer $i\omega_m$ from an initial state with momentum \mathbf{k} is described by Eq. 8. Continuing the RPA scheme by expanding to second order in the gauge fields and summing over momenta, which accounts for the polarization bubble, yields the correction

$$\Delta S = -\frac{1}{2} \sum_{\omega_m} \int \frac{d^2 q}{(2\pi)^2} \sum_{s,s' \in \{1,2\}} \sum_{\mu,\nu \in \{0,1\}} a_\mu^{(s)}(\mathbf{q}, i\omega_m) \Pi_{\mu\nu}(\mathbf{q}, i\omega_m) \delta_{ss'} a_\nu^{(s')}(-\mathbf{q}, -i\omega_m), \quad (11)$$

$$\Pi_{00}(\mathbf{q}, i\omega_m) = T \sum_{\epsilon_n} \int \frac{d^2 k}{(2\pi)^2} G(\mathbf{k} + \mathbf{q}, i\epsilon_n + i\omega_m) G(\mathbf{k}, i\epsilon_n) = -\int \frac{d^2 k}{(2\pi)^2} \frac{f(\xi_{\mathbf{k}+\mathbf{q}}) - f(\xi_{\mathbf{k}})}{i\omega_m - \xi_{\mathbf{k}+\mathbf{q}} + \xi_{\mathbf{k}}}, \quad (12)$$

$$\Pi_{01}(\mathbf{q}, i\omega_m) = \Pi_{10}(\mathbf{q}, i\omega_m) = 0, \quad (13)$$

$$\Pi_{11}(\mathbf{q}, i\omega_m) = \frac{T}{m^*} \sum_{\epsilon_n} \int \frac{d^2 k}{(2\pi)^2} G(\mathbf{k}, i\epsilon_n) - T \sum_{\epsilon_n} \int \frac{d^2 k}{(2\pi)^2} \frac{\hat{\mathbf{q}} \times \mathbf{k}}{m^*} \cdot \frac{(-\hat{\mathbf{q}}) \times \mathbf{k}}{m^*} G(\mathbf{k} + \mathbf{q}, i\epsilon_n + i\omega_m) G(\mathbf{k}, i\epsilon_n) = \\ = \frac{n_e}{m^*} - \int \frac{d^2 k}{(2\pi)^2} \left(\frac{\hat{\mathbf{q}} \times \mathbf{k}}{m^*} \right)^2 \frac{f(\xi_{\mathbf{k}+\mathbf{q}}) - f(\xi_{\mathbf{k}})}{i\omega_m - \xi_{\mathbf{k}+\mathbf{q}} + \xi_{\mathbf{k}}}, \quad (14)$$

with $f(\xi) = \frac{1}{\exp(\xi/T)+1}$ the Fermi distribution function. Note that in principle, if a superconducting gap opens in the spectrum, the polarization bubble needs to be re-computed accounting for this gap. If we work close to the superconducting transition, this can be ignored. The integrals in Eqs. 12–14 are explicitly evaluated in the zero-temperature case by Isobe and Fu [53], for example. While not immediately obvious from the definition Eqs. 12–14, $\Pi_{\mu\nu}(\mathbf{q}, i\omega_m)$ is rotationally invariant, depending only on the magnitude of \mathbf{q} . With this, the effective action for the gauge field within the RPA is

$$S_{\text{eff}}[a_\mu] = \frac{1}{2} \sum_{\omega_m} \int \frac{d^2q}{(2\pi)^2} \sum_{s,s' \in \{1,2\}} \sum_{\mu,\nu \in \{0,1\}} a_\mu^{(s)}(\mathbf{q}, i\omega_m) [\mathcal{D}^{\text{RPA}}(q, i\omega_m)]_{\mu s, \nu s'}^{-1} a_\nu^{(s')}(-\mathbf{q}, -i\omega_m), \quad (15)$$

$$[\mathcal{D}^{\text{RPA}}(q, i\omega_m)]_{\mu s, \nu s'}^{-1} = [\mathcal{D}^{(0)}(q, i\omega_m)]_{\mu s, \nu s'}^{-1} - \Pi_{\mu\nu}(q, i\omega_m) \delta_{ss'}. \quad (16)$$

To implement the MRPA correction on top of this, we first need to find the RPA fermion polarization function [9],

$$[K^{\text{RPA}}(q, i\omega_m)]_{\mu s, \nu s'}^{-1} = [\Pi(q, i\omega_m)]_{\mu\nu}^{-1} \delta_{ss'} - \mathcal{D}_{\mu s, \nu s'}^{(0)}(q, i\omega_m). \quad (17)$$

The MRPA prescription is to replace K^{RPA} by K^{MRPA} , which is defined in imaginary time as

$$[K^{\text{MRPA}}(q, i\omega_m)]_{\mu s, \nu s'}^{-1} = [K^{\text{RPA}}(q, i\omega_m)]_{\mu s, \nu s'}^{-1} + \mathcal{F}_{1, \mu\nu}(q, i\omega_m) \delta_{ss'} \quad (18)$$

$$\mathcal{F}_{1, \mu\nu} = \frac{m^* - m_b}{e^2 n_e} \begin{pmatrix} \frac{\omega_m^2}{q^2} & 0 \\ 0 & -1 \end{pmatrix}_{\mu\nu} \quad (19)$$

where K^{RPA} is calculated with the effective mass m^* . Here, we make a distinction between the interaction-renormalized effective mass m^* and the bare band mass m_b . The effective mass is set by the interaction scale so that $\hbar^2/m^* = Ce^2\ell_B/\epsilon$ with ϵ the dielectric constant and C a constant estimated[6] to be roughly $C = 0.3$. The MRPA is designed to satisfy Kohn's theorem and the f-sum rule, which are defined in terms of the bare mass m_b rather than the effective mass [9]. From Eq. 16 and Eq. 17, we may infer the relationship between K^{RPA} and \mathcal{D}^{RPA} (sum over repeated indices implied – Greek alphabet letters are indices of gauge field components, Latin alphabet letters are layer indices)

$$\mathcal{D}_{\mu s, \nu s'}^{\text{RPA}}(q, i\omega_m) = \mathcal{D}_{\mu s, \nu s'}^{(0)}(q, i\omega_m) + \mathcal{D}_{\mu s, \sigma t}^{(0)}(q, i\omega_m) K_{\sigma t, \rho u}^{\text{RPA}}(q, i\omega_m) \mathcal{D}_{\rho u, \nu s'}^{(0)}(q, i\omega_m). \quad (20)$$

To get the MRPA gauge propagator, $\mathcal{D}^{\text{MRPA}}$, we simply replace K^{RPA} in Eq. 20 with K^{MRPA} .

Since $\mu, \nu \in \{0, 1\}$ and $s, s' \in \{1, 2\}$, the propagators are 4x4 matrices. From here on, we assume that at least one layer is taken to be CE's, so we may set $c_2 = 1$ in Eq. 1. We define the in-phase and out-of-phase components of the gauge field as

$$\begin{aligned} a_0^+ &= \frac{1}{\sqrt{2}} (c_1 a_0^{(1)} + a_1^{(2)}), & a_1^+ &= \frac{1}{\sqrt{2}} (a_0^{(1)} + a_1^{(2)}), \\ a_0^- &= \frac{1}{\sqrt{2}} (c_1 a_0^{(1)} - a_1^{(2)}), & a_1^- &= \frac{1}{\sqrt{2}} (a_0^{(1)} - a_1^{(2)}). \end{aligned} \quad (21)$$

With these components, both the gauge propagators and fermion polarization matrices are block diagonal. In this form, the bare gauge propagator is

$$\mathcal{D}^{(0)}(q, i\omega_m)^{-1} = \begin{pmatrix} \mathcal{D}_{+, \mu\nu}^{(0)}(q, i\omega_m)^{-1} & 0 \\ 0 & \mathcal{D}_{-, \mu\nu}^{(0)}(q, i\omega_m)^{-1} \end{pmatrix}_{\mu\nu}, \quad (22)$$

$$\mathcal{D}_{\pm, \mu\nu}^{(0)}(q, i\omega_m)^{-1} = \begin{pmatrix} 0 & \frac{q}{4\pi} \\ \frac{q}{4\pi} & -\frac{q^2}{(4\pi)^2} (V_{11}(q) \pm V_{12}(q)) \end{pmatrix}_{\mu\nu}. \quad (23)$$

At RPA and MRPA level we then have

$$\text{RPA: } \mathcal{D}_{\pm, \mu\nu}^{\text{RPA}}(q, i\omega_m) = \mathcal{D}_{\pm, \mu\nu}^{(0)}(q, i\omega_m) + \mathcal{D}_{\pm, \mu\sigma}^{(0)}(q, i\omega_m) \left((\Pi(q, i\omega_m))^{-1} - \mathcal{D}_{\pm}^{(0)}(q, i\omega_m) \right)_{\sigma\rho}^{-1} \mathcal{D}_{\pm, \rho\nu}^{(0)}(q, i\omega_m), \quad (24)$$

$$\begin{aligned} \text{MRPA: } \mathcal{D}_{\pm, \mu\nu}^{\text{MRPA}}(q, i\omega_m) &= \\ &= \mathcal{D}_{\pm, \mu\nu}^{(0)}(q, i\omega_m) + \mathcal{D}_{\pm, \mu\sigma}^{(0)}(q, i\omega_m) \left((\Pi(q, i\omega_m))^{-1} - \mathcal{D}_{\pm}^{(0)}(q, i\omega_m) + \mathcal{F}_1(q, i\omega_m) \right)_{\sigma\rho}^{-1} \mathcal{D}_{\pm, \rho\nu}^{(0)}(q, i\omega_m). \end{aligned} \quad (25)$$

In order to convert back to the original $a^{(s)}$ basis, we may use the identities

$$\mathcal{D}_{\pm,\mu\nu} = \langle a_{\mu}^{\pm}(q, i\omega_m) a_{\nu}^{\pm}(-q, -i\omega_m) \rangle, \quad (26)$$

$$\mathcal{D}_{\mu s, \nu s'} = \langle a_{\mu}^{(s)}(q, i\omega_m) a_{\nu}^{(s')}(-q, -i\omega_m) \rangle, \quad (27)$$

along with the transformation Eq. 21. We note that in block-diagonal form, the propagators are identical between the CE-CE ($c_1 = 1$) and CE-CH ($c_1 = -1$) systems. The physics remains different however due to the different transformations Eq. 21 from the block-diagonal form into the physical layer basis.

B. The effective interaction

The gauge field mediates interaction between the fermions. Looking at the form of interactions between a and ψ in Eq. 7 and Eq. 8, we can see that the effective interaction includes terms of the form

$$\mathcal{V} = -\frac{1}{2} \sum_{s, s' \in \{1, 2\}} \sum_{\mu, \nu \in \{0, 1\}} M_{\mu\nu}(\mathbf{k}, \mathbf{k}', \hat{\mathbf{q}}) \mathcal{D}_{\mu s, \nu s'}^{(M)\text{RPA}}(\mathbf{q}, i\omega_m) \psi_s^{\dagger}(\mathbf{k} + \mathbf{q}, i\epsilon_n + i\omega_m) \psi_s(\mathbf{k}, i\epsilon_n) \psi_{s'}^{\dagger}(\mathbf{k}' + \mathbf{q}, i\epsilon_n - i\omega_m) \psi_{s'}(\mathbf{k}', i\epsilon_n), \quad (28)$$

$$M_{\mu\nu}(\mathbf{k}, \mathbf{k}', \hat{\mathbf{q}}) = \frac{1}{2} \begin{pmatrix} 1 & -i \frac{\hat{\mathbf{z}} \cdot (\hat{\mathbf{q}} \times \mathbf{k}')}{m^*} \\ i \frac{\hat{\mathbf{z}} \cdot (\hat{\mathbf{q}} \times \mathbf{k})}{m^*} & \frac{(\hat{\mathbf{q}} \times \mathbf{k}) \cdot (\hat{\mathbf{q}} \times \mathbf{k}')}{m^{*2}} \end{pmatrix}. \quad (29)$$

The form of these terms may be derived by computing the expectation value of e^{-S} for the action Eq. 1, using the MRPA value of the gauge field propagator, Eqs. 25–27. This step follows Isobe-Fu [53] exactly.

C. Eliashberg theory

Following [53] we write the Eliashberg equations for the quasiparticle residue $Z_m = Z(i\epsilon_m)$ and the anomalous self-energy $\phi_m^{(l)}$ in the angular momentum l pairing channel as

$$(1 - Z_n)\epsilon_n = -T \sum_m \int \frac{d^2q}{(2\pi)^2} \frac{Z_{n+m}(\epsilon_n + \omega_m)}{Z_{n+m}^2(\epsilon_n + \omega_m)^2 + \xi_{\mathbf{k}+\mathbf{q}}^2 + |\phi_{n+m}^{(l)}|^2} V_{\text{ex}}(\mathbf{k}, \mathbf{q}, i\omega_m) \quad (30)$$

$$\phi_n^{(l)} e^{il\theta_{\mathbf{k}}} = -T \sum_m \int \frac{d^2q}{(2\pi)^2} \frac{\phi_{n+m}^{(l)} e^{il\theta_{\mathbf{k}+\mathbf{q}}}}{Z_{n+m}^2(\epsilon_n + \omega_m)^2 + \xi_{\mathbf{k}+\mathbf{q}}^2 + |\phi_{n+m}^{(l)}|^2} V_{\text{c}}(\mathbf{k}, \mathbf{q}, i\omega_m) \quad (31)$$

where

$$V_{\text{ex}}(\mathbf{k}, \mathbf{q}, i\omega_m) = - \sum_{\mu, \nu} M_{\mu\nu}(\mathbf{k}, \mathbf{k} + \mathbf{q}, \hat{\mathbf{q}}) \sum_{s \in \{1, 2\}} \mathcal{D}_{\mu s, \nu s}(q, i\omega), \quad (32)$$

$$V_{\text{c}}(\mathbf{k}, \mathbf{q}, i\omega_m) = - \sum_{\mu, \nu} M_{\mu\nu}(\mathbf{k}, -\mathbf{k} - \mathbf{q}, \hat{\mathbf{q}}) \sum_{s \in \{1, 2\}} \mathcal{D}_{\mu s, \nu \bar{s}}(q, i\omega), \quad (33)$$

with \bar{s} the opposite layer to s . Here $\epsilon_n = (2n+1)\pi T$ is a fermionic Matsubara frequency and $\omega_m = 2m\pi T$ is a bosonic Matsubara frequency.

Eqs. 30–31 are similar to the Eliashberg equations for typical phonon driven superconductivity[60]. In that case there is usually a natural small parameter which is the phonon energy scale divided by the Fermi energy. Given this small parameter one can make the approximation that

$$Z_{n+m}^2(\epsilon_n + \omega_m)^2 + |\phi_{n+m}^{(l)}|^2 \ll \xi_{\mathbf{k}+\mathbf{q}}^2 \quad (34)$$

and the denominator becomes a delta function $\delta(\xi_{\mathbf{q}+\mathbf{k}})$ restricting the q integral to the Fermi surface. This assumption is also made by [18, 49, 53, 54, 56] for the quantum Hall bilayer, although it is harder to justify. As we will discuss further in section V below, this assumption is rather dangerous in the quantum Hall bilayer case and can give some spurious results and it is important to be careful to distinguish which results are robust and which results are a property of the approximation. Note that Ref. [49] does correctly point out the danger of this assumption but

they make the assumption nonetheless, as will we for much of this work (however, see the more detailed discussion of section V).

At this stage we will still follow [18, 49, 53, 54, 56] and make the assumption Eq. 34, reconsidering it only in section V. Thus we obtain

$$(1 - Z_n)\epsilon_n = -\pi T \sum_m \frac{Z_{n+m}(\epsilon_n + \omega_m)}{\sqrt{Z_{n+m}^2(\epsilon_n + \omega_m)^2 + |\phi_{n+m}^{(l)}|^2}} \lambda_Z(\omega_m), \quad (35)$$

$$\phi_n^{(l)} e^{il\theta_{\mathbf{k}}} = -\pi T \sum_m \frac{\phi_{n+m}^{(l)} e^{il\theta_{\mathbf{k}+\mathbf{q}}}}{\sqrt{Z_{n+m}^2(\epsilon_n + \omega_m)^2 + |\phi_{n+m}^{(l)}|^2}} \lambda_\phi^{(l)}(\omega_m) \quad (36)$$

where the coupling constants $\lambda_Z(\omega_m)$ and $\lambda_\phi^{(l)}(\omega_m)$ are given by

$$\lambda_Z(\omega_m) = \int \frac{d^2q}{(2\pi)^2} \delta(\xi_{\mathbf{k}+\mathbf{q}}) V_{\text{ex}}(\mathbf{k}, \mathbf{q}, i\omega_m), \quad (37)$$

$$\lambda_\phi^{(l)}(\omega_m) = \int \frac{d^2q}{(2\pi)^2} \delta(\xi_{\mathbf{k}+\mathbf{q}}) V_c(\mathbf{k}, \mathbf{q}, i\omega_m) \left(1 + \frac{q}{k_F} e^{il(\theta_{\mathbf{q}} - \theta_{\mathbf{k}})}\right)^l. \quad (38)$$

The angular parts of these integrals may be performed analytically, to yield [53], [56]

$$\lambda_Z(\omega_m) = \frac{1}{(2\pi)^2} \frac{m^*}{k_F} \int_0^{2k_F} dq \left\{ -\frac{1}{\sqrt{1 - \left(\frac{q}{2k_F}\right)^2}} [\mathcal{D}_{+,00}(q, i\omega_m) + \mathcal{D}_{-,00}(q, i\omega_m)] \right. \\ \left. - \frac{k_F^2}{m^{*2}} \sqrt{1 - \left(\frac{q}{2k_F}\right)^2} [\mathcal{D}_{+,11}(q, i\omega_m) + \mathcal{D}_{-,11}(q, i\omega_m)] \right\} \quad (39)$$

$$\lambda_\phi^{(l)}(\omega_m) = \frac{1}{(2\pi)^2} \frac{m^*}{k_F} \int_0^{2k_F} \left\{ \frac{1}{\sqrt{1 - \left(\frac{q}{2k_F}\right)^2}} \cos\left(2l \sin^{-1} \frac{q}{2k_F}\right) c_1 [\mathcal{D}_{+,00}(q, i\omega_m) - \mathcal{D}_{-,00}(q, i\omega_m)] \right. \\ \left. + \frac{k_F}{m^*} \sin\left(2l \sin^{-1} \frac{q}{k_F}\right) (1 + c_1) [\mathcal{D}_{+,01}(q, i\omega_m) - \mathcal{D}_{-,01}(q, i\omega_m)] \right. \\ \left. - \frac{k_F^2}{m^{*2}} \sqrt{1 - \left(\frac{q}{2k_F}\right)^2} \cos\left(2l \sin^{-1} \frac{q}{2k_F}\right) [\mathcal{D}_{+,11}(q, i\omega_m) - \mathcal{D}_{-,11}(q, i\omega_m)] \right\}. \quad (40)$$

In our calculations, we use the MRPA result for the propagator. In the CE-CH case, $c_1 = -1$, the second term in Eq. 40 is zero, so as mentioned in [56] for the RPA, the CE-CH pairing for l and $-l$ is of equal strength, and this is also true at MRPA level. We note that $\lambda_Z(\omega_m)$ does not depend on c_1 , so it will be exactly equal for CE-CE and CE-CH couplings: only $\lambda_\phi^{(l)}(\omega_m)$ changes based on which coupling is used.

This concludes a brief overview of the CSMRPAE theory — we may use Eqs. 25, 39, 40 to compute the Eliashberg coupling constants. Results are shown in Fig. 1 of the main text and in Section VII.

D. Why not go to MMRPA?

The MMRPA is an additional correction above the MRPA [9]. In MMRPA, magnetic flux is attached to the composite fermions, recovering the physics of the particles undertaking cyclotron motion and therefore carrying orbital magnetization, which is lost in the mean-field approximation. We choose to not apply that correction here: the MMRPA is designed to study the response to the *external* gauge field, A_μ , but we are really interested in the response to fluctuations of the *statistical* gauge field, a_μ . Microscopic insight into how cyclotron motion gives rise to additional currents and changes the effective external field may be used to develop the MMRPA as a response to the external gauge field, but such arguments do not necessarily apply to the statistical gauge field. For this reason, we believe the MMRPA to not be an appropriate correction in this computation. A second way to justify our choice is to state that we are pairing fermions that are undressed of their orbital angular momentum.

IV. DIFFERENT DIVERGENCES IN CE-CE PAIRING VERSUS CE-CH PAIRING WHEN EVALUATED IN RPA OR NONZERO m_b MRPA

In this section we look at the RPA calculations of Isobe-Fu[53] and Rüegg-Chaudhary-Slager[56] and show that, while the divergent terms for the quasiparticle residue coupling constants λ_Z are equal between the two cases (CE-CE vs CE-CH), the divergent terms in the pairing coupling constants λ_ϕ differ. Thus any comparison between the strength of the two pairing instabilities will depend on the cutoff prescription. We also show that the divergent terms are still present in the MRPA if $m_b > 0$, and disappear as a power of m_b , meaning there are no cutoff-based issues in the $m_b = 0$ MRPA. We formally work in the MRPA, noting that the RPA may be recovered exactly by setting $m_b = m^*$.

Isobe and Fu [53] observe that the Eliashberg couplings λ_Z and λ_ϕ diverge as a function of the low-momentum cutoff, q_c , with $\lambda_Z \propto 1/q_c$ and $\lambda_\phi \propto \log q_c$. We show that these divergences are multiplied by a power of m_b , meaning they go away in the limit $m_b \rightarrow 0$. In this section we focus on the low-momentum limit, $q \ll k_F$, but allow ω_m to take any value. We choose units with $k_F = 1$ and $e = 1$. In this limit [53], we have

$$\Pi_{00}(q, i\omega_m) \approx -\frac{\epsilon_F}{2\pi} \frac{q^2}{\omega_m^2} (1 + \mathcal{O}(q^2/\omega_m^2)) \quad (41)$$

$$\Pi_{11}(q, i\omega_m) \approx \frac{\epsilon_F}{2\pi} (1 + \mathcal{O}(q^2/\omega_m^2)) \quad (42)$$

From Eq. 17–19, we get

$$(K_{\pm}^{\text{MRPA}}(q, i\omega_m))_{\mu\nu}^{-1} = \begin{pmatrix} -\frac{2\pi}{\epsilon_F} \frac{\omega_m^2}{q^2} & 0 \\ 0 & \frac{2\pi}{\epsilon_F} \end{pmatrix} (1 + \mathcal{O}(q^2)) - \begin{pmatrix} V_{\pm}(q) & \frac{4\pi}{q} \\ \frac{4\pi}{q} & 0 \end{pmatrix} + \frac{m^* - m_b}{n_e} \begin{pmatrix} \frac{\omega_m^2}{q^2} & 0 \\ 0 & -1 \end{pmatrix} \quad (43)$$

where $V_{\pm}(q) = V_{11}(q) \pm V_{12}(q)$. Using that $k_F = 1$, we have $n_e = 1/4\pi$ and $\epsilon_F = 1/2m^*$. This implies

$$K_{\pm, \mu\nu}^{\text{MRPA}}(q, i\omega_m) = \frac{-1}{\frac{(4\pi)^2}{q^2} + 4\pi\tilde{m}_b [V_{\pm}(q) + 4\pi\tilde{m}_b \frac{\omega_m^2}{q^2}]} \begin{pmatrix} 4\pi\tilde{m}_b & \frac{4\pi}{q} \\ \frac{4\pi}{q} & -4\pi\tilde{m}_b \frac{\omega_m^2}{q^2} - V_{\pm}(q) \end{pmatrix}, \quad (44)$$

where $\tilde{m}_b = m_b + m^*\mathcal{O}(q^2)$, due to the inaccuracy in our approximation of Π .

Using Eq. 20, we get

$$\mathcal{D}_{\pm, \mu\nu}^{\text{MRPA}}(q, i\omega_m) = \frac{1}{(4\pi)^2 + 4\pi\tilde{m}_b [q^2 V_{\pm}(q) + 4\pi\tilde{m}_b \omega_m^2]} \begin{pmatrix} V_{\pm}(q)(4\pi\tilde{m}_b \omega_m)^2 + 4\pi\tilde{m}_b \omega_m^2 \frac{(4\pi)^2}{q^2} & \frac{4\pi}{q} (4\pi\tilde{m}_b \omega_m)^2 \\ \frac{4\pi}{q} (4\pi\tilde{m}_b \omega_m)^2 & 0 \end{pmatrix} + \mathcal{O}(1). \quad (45)$$

When computing λ_Z from Eq. 39 we are concerned with terms of the type $\mathcal{D}_{+, \mu\nu}^{\text{MRPA}} + \mathcal{D}_{-, \mu\nu}^{\text{MRPA}}$, which can be approximated to lowest two orders in q as

$$\begin{aligned} & \mathcal{D}_{+, \mu\nu}^{\text{MRPA}}(q, i\omega_m) + \mathcal{D}_{-, \mu\nu}^{\text{MRPA}}(q, i\omega_m) = \\ & = \frac{2}{(4\pi)^2 [1 + \tilde{m}_b^2 \omega_m^2]} \begin{pmatrix} V_{11}(q)(4\pi m_b \omega_m)^2 + 4\pi m_b \omega_m^2 \frac{(4\pi)^2}{q^2} & \frac{4\pi}{q} (4\pi m_b \omega_m)^2 \\ \frac{4\pi}{q} (4\pi m_b \omega_m)^2 & 0 \end{pmatrix} + \mathcal{O}(1) \end{aligned} \quad (46)$$

Since $\tilde{m}_b = m_b + \mathcal{O}(m^*q^2)$, the most divergent term is $\tilde{m}_b/q^2 = m_b/q^2 + \mathcal{O}(1)$, and we may simply replace all the \tilde{m}_b by m_b . The leading order divergence in \mathcal{D}_{00} is discussed in Section VI-C of [6]. See section V below for a more detailed discussion of this divergence and the comparison with the discussion of Halperin-Lee-Read[6]. Equation 39 shows that for momentum cutoff q_c ,

$$\lambda_Z \approx A \frac{m_b \omega_m^2}{1 + m_b^2 \omega_m^2} \frac{1}{q_c} + B \frac{m_b^2 \omega_m^2}{1 + m_b^2 \omega_m^2} \log q_c + \mathcal{O}(q_c^0), \quad (47)$$

with A, B being $\mathcal{O}(1)$ constants. Note that in these units, $\omega_c = 1/m_b$. At a given frequency, when $m_b \rightarrow 0$, there is no divergence in λ_Z . At finite m_b , the leading divergence is $\sim 1/q_c$, with the strength proportional to m_b when $\omega_m \ll \omega_c = 1/m_b$, but proportional to $1/m_b$ when $\omega_m \gg \omega_c = 1/m_b$.

To compute $\lambda_\phi^{(l)}$ via Eq. 40, we need to evaluate terms of the type $\mathcal{D}_{+, \mu\nu}^{\text{MRPA}} - \mathcal{D}_{-, \mu\nu}^{\text{MRPA}}$. Again approximating up to zeroth order in q , we find (since $V_{12} \sim 1/q$ at small q)

$$\begin{aligned} & \mathcal{D}_{+, \mu\nu}^{\text{MRPA}}(q, i\omega_m) - \mathcal{D}_{-, \mu\nu}^{\text{MRPA}}(q, i\omega_m) = \\ & = \frac{2(\tilde{m}_b \omega_m)^4}{[1 + \tilde{m}_b^2 \omega_m^2]^2} \begin{pmatrix} V_{12}(q) & 0 \\ 0 & 0 \end{pmatrix} + \mathcal{O}(1) \end{aligned} \quad (48)$$

The most divergent term is $\sim 1/q$, so replacing \tilde{m}_b with m_b only introduces an error $\mathcal{O}(q)$. With a momentum cutoff q_c , we get from Eq. 40

$$\lambda_\phi^{(l)} \approx c_1 C \frac{m_b^4 \omega_m^4}{(1 + m_b^2 \omega_m^2)^2} \log q_c + \mathcal{O}(1), \quad (49)$$

with C a $\mathcal{O}(1)$ constant. So the leading logarithmic divergence goes away as $m_b \rightarrow 0$. At finite m_b , the strength of the divergence is $\sim m_b^4 \omega_m^4 = (\omega_m/\omega_c)^4$ when $\omega_m m_b = \omega_m/\omega_c \ll 1$: in the opposite limit $\omega_m m_b \gg 1$, we have $\lambda_\phi^{(l)} \approx c_1 C \log q_c + \mathcal{O}(1)$. The important part of the result Eq. 49 is that the divergent term is independent of l , but is dependent on c_1 , i.e., on the type of coupling: it is positive for CE-CE, but negative for CE-CH. This confirms, as suggested by Isobe-Fu [53] that for CE-CE coupling, different- l channels may be compared by introducing a cutoff, as the divergent terms are equal anyway. The same holds for different l -channels of CE-CH, but does not hold for comparing CE-CE to CE-CH. In the case of comparing CE-CE to CE-CH, the divergent terms are different (in fact exactly opposite) so the couplings may not be compared directly in a meaningful way, unlike what is claimed in [56]. This analytically supports the numerical results shown in Fig. 3 of Section II, where the ordering in strength of the coupling channels and the difference between their strengths depends on the cutoff choice. The only case where a CE-CE to CE-CH comparison is meaningful is when $m_b \rightarrow 0$ where the divergence disappears.

V. DETAILED ANALYSIS OF DIVERGENCES, EVEN AT VERY HIGH ω_m

We have successfully eliminated divergences that stem from the cyclotron mode, by pushing the cyclotron mode off to infinity in the $m_b \rightarrow 0$ limit. One might worry whether, no matter how large the cyclotron scale is, divergences at (or above) that scale may be problematic. This potential concern encouraged us to look more closely at these divergences.

First, we find that the divergences obtained by the approaches of Refs. [18, 53, 56], (i.e., all cases of divergences by prior groups mentioned in the main text) are greatly exaggerated by details of the approximation method used. A more careful evaluation of the Eliashberg equations shows that for nonzero value of m_b the divergence of the nonanomalous self-energy stemming from the cyclotron mode is actually only $\log q_c$ not $1/q_c$. Furthermore, this log divergence is precisely the ultraviolet divergence discussed in detail by Halperin-Lee-Read[6] (section VI.C) which stems from the vanishing overlap between wavefunctions with and without the singular gauge transformation. This type of divergence can be fairly safely ignored, as it has been in the past[6]. A similar analysis shows that the anomalous part of the self-energy is actually not divergent at all. With this revised understanding of the divergences in mind, we expect that pushing the cyclotron frequency up to infinite energy should leave us with a well behaved low energy theory.

Roughly, the error by prior works[18, 53, 56] in evaluation of the infrared divergences stems from the restriction of a momentum integral in the self-energy to lie precisely on the Fermi surface. For the non-anomalous self-energy this gives a divergent one-dimensional integral $\int_{q_c} dq V_{ex}(q) \sim 1/q_c$ where $V_{ex} \sim 1/q^2$ is the most singular part of the gauge interaction. However, the integral is not really one-dimensional, but rather is an integral over a strip near the Fermi surface whose width is set by a (potentially small but) finite energy scale related to the frequency scale of the pairing attraction. At small enough q this integral should always be treated as two-dimensional yielding instead $\int_{q_c} d^2q V_{ex}(q) \sim \log q_c$, a much less serious divergence, and as mentioned above, one that we understand well[6]. Using a similar analysis, the divergence in the anomalous self-energy was previously described as a one dimensional integral $\int_{q_c} dq V_c(q) \sim \log q_c$ where $V_c \sim 1/q$. Again the divergence comes from treating the integral as strictly one-dimensional, whereas a more proper two-dimensional treatment finds the integral $\int_{q_c} d^2q V_c(q)$ to be non-divergent.

Let us now take a more detailed look at some of these divergences for nonzero m_b . Before so doing, we should recall the derivation of the coupling constants Eqs. 37-38. Note in particular that we have used inequality Eq. 34 to restrict the integration to the Fermi surface. However, the left hand side of this inequality is never arbitrarily small, so the resulting delta-function obtained in Eqs. 37-38 is never infinitely sharp. In fact, we should think of the delta function $\delta(\xi_{\mathbf{q}+\mathbf{k}})$ as having a thickness of

$$\delta\xi_{n,m} = \sqrt{Z_{n+m}^2 (\epsilon_n + \omega_m)^2 + |\phi_{n+m}^{(l)}|^2}$$

or equivalently the distance perpendicular from the Fermi surface is smeared by

$$\delta Q_{\perp,n,m} = \frac{1}{v_F} \sqrt{Z_{n+m}^2 (\epsilon_n + \omega_m)^2 + |\phi_{n+m}^{(l)}|^2}$$

with v_F the Fermi velocity. For q greater than this scale, we should think of the q integral in Eqs. 37-38 as being one-dimensional as we have done in Eqs. 39-40. However, for q smaller than this scale the q integral should be thought

of as being two-dimensional. For each value of n and m in Eqs. 30-31 this cutoff scale is different, however, it is always nonzero for any finite T or ω_m .

This analysis suggests it should be possible to pursue Eliashberg Chern-Simons theory without serious divergences even for nonzero values of m_b , although this would require a more careful analysis of the relevant two-dimensional integrals, which is beyond the scope of this work. Instead we focus in this work on the $m_b \rightarrow 0$ limit such that all problematic divergences are pushed away to infinite frequencies and we can safely work with the one-dimensional Fermi surface integrals.

VI. COMMENTS ON CHERN-SIMONS THEORY AND LANDAU LEVEL PROJECTION

The Chern-Simons fermion (CE) approach to fractional quantum Hall effects[6, 61] begins by making a singular gauge transformation that then represents each electron as a fermion bound to an even number of (Chern-Simons) flux quanta. This transformation (sometimes called a Chern-Simons transformation) is exact. Once one makes the exact transformation, one is typically forced to make a mean field approximation of some sort, and then attempt to include the effects of fluctuations around mean field using approaches such as RPA. It is at the mean-field step that the calculation is no longer exact. Nonetheless, we may hope that an approach to including fluctuations, such as MRPA[9, 57] may still describe the physics, at least roughly, for any value of m_b (which we treat as a separate parameter from m^* which is set by the interaction scale). In particular, we may hope that in the limit of m_b going to zero we would at least roughly represent the physics restricted to the lowest Landau level (this has been tested with good results, for example, in Ref. [62]), and for finite m_b we would expect the MRPA to incorporate the effects of Landau level mixing.

The idea of attaching Chern-Simons flux to *holes* within the lowest Landau level (CH) was suggested, and derived, by Ref. [10]. While the resulting field theory seems valid as a low energy long wavelength description, it is not on the same footing as the above CE Chern-Simons approach, which is in principle an exact description before the mean-field approximation is made. The CH model is not exact in the same way since one cannot even define a hole degree of freedom except within the finite dimensional Hilbert space of a single Landau level. Further, once we project to a single Landau level, if we try to make the exact singular gauge transformation, the system would no longer remain within that Landau level. (We note in passing that for a fractional Chern insulator with finite dimensional Hilbert space, one could in principle attach flux to holes in a well-defined way without any projection to a single band. However, this would not result in the correct mean field state that we want for the CH Fermi liquid.)

The CH model is strictly equivalent to a physical system of charge $+e$ fermions (compared to charge $-e$ electrons) in a magnetic field. When projected to a single Landau level, the CH model is equivalent to a theory of holes in the single Landau level of electrons (which is why we use this model). However, when Landau level mixing is included, the system of charge $+e$ fermions and the system of charge $-e$ electrons are inequivalent.

As mentioned above, in the limit that m_b is taken to zero, and one can think of the system of being projected to a single Landau level and the concept of particle-hole conjugation is well defined within the Hilbert space of the single Landau level. In this case, the CH MRPA theory also becomes an equally good description of the system as the CE MRPA.

VII. FAVOURED CHANNELS FOR CE-CE AND CE-CH PAIRING IN MRPA CHERN-SIMONS ELIASHBERG THEORY

We evaluate the pairing Eliashberg constants $\lambda_\phi^{(l)}(\omega_m)$ by numerically integrating Eq. 40 within the MRPA with $m_b = 0$, using Eq. 25 for the gauge propagator $\mathcal{D}_{\mu\nu}$. Note that as there is no divergence now, there is no need to introduce a cutoff. The results in Fig. 4 show that for CE-CE coupling, $l = 1$ is now favoured unambiguously. Even if d is made larger, or the frequency range extended, $l = 1$ is always the strongest coupling, unlike in the RPA results presented in Section I. Another important thing to note is that $\lambda_\phi^{(l)}(\omega_m) \rightarrow 0$ always for $\omega \gg \epsilon_F$. With RPA we would have $\lambda_\phi^{(l)}(\omega_m) > 0$ for CE-CE and $\lambda_\phi^{(l)}(\omega_m) < 0$ for CE-CH at high frequency, as discussed in section VIII.

As evident from Eq. 40, l and $-l$ are degenerate for CE-CH coupling. For CE-CE coupling $l = 0$ and $l = 2$ are similar in strength, both similar to $l = 1$ in CE-CH, and in CE-CE, $l = -1$ is similar in strength to $l = 3$, both similar to CE-CH $l = 2$. If the coupling were exactly symmetric between CE-CE and CE-CH, we would expect $(l + 1)$ -wave of CE-CE to coincide with l -wave of CE-CH, coinciding with the $-l$ -wave CE-CH and $(-l + 1)$ -wave CE-CE too. We see this degeneracy only approximately. If the adjustment of Section VIII D is made to the MRPA, these quadruplets are exactly degenerate in strength.

By far the most precise degeneracy is seen between $l = 0$ CE-CH and $l = 1$ CE-CE, as shown in Fig. 4: the coupling strengths follow each other closely, with the CE-CH $l = 0$ being very slightly stronger. The difference seen here is

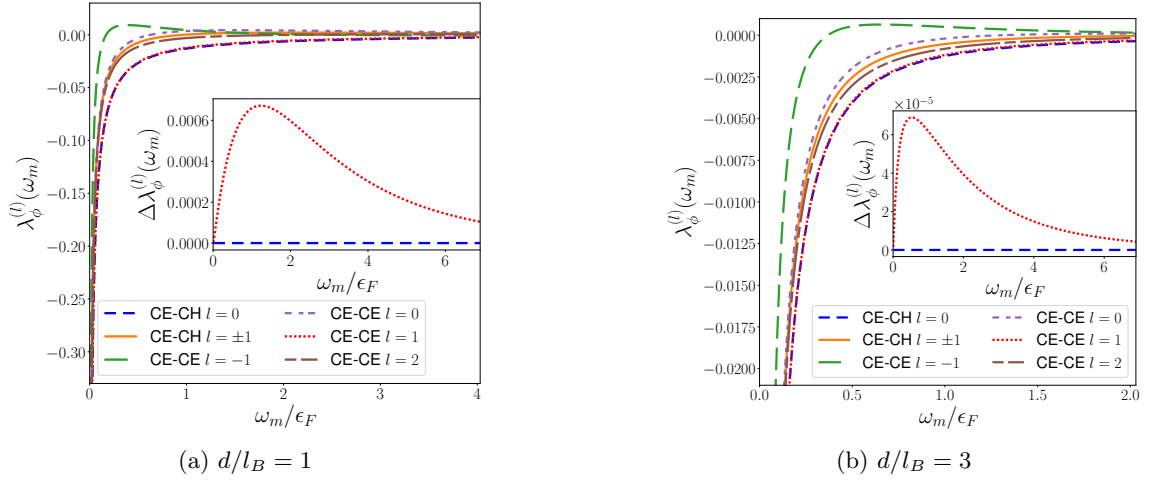


FIG. 4. The results for $\lambda_\phi^{(l)}(\omega_m)$ within the $m_b = 0$ MRPA, showing unambiguous results for a large range of ω_m for two different values of d/l_B . In CE-CE coupling, $l = 1$ is always favoured, and in CE-CH coupling, $l = 0$ is favoured. The two are very similar, but not exactly equal in strength. The insets show the difference between them, magnified.

over 2 orders of magnitude smaller than the difference seen within the RPA in [56]. The difference is sufficiently small that we do not believe it is physically meaningful, given the rough level of this calculation.

In short: numerical integration of Eq. 40 shows that $l = 1$ is unambiguously favoured for CE-CE coupling, and confirms that $l = 0$ is favoured for CE-CH coupling. It also shows that the two are extremely similar, but not precisely equal in strength.

VIII. COMPARISON OF $l = 0$ CE-CH AND $l = 1$ CE-CE AND A POSSIBLE ADJUSTMENT TO THE MRPA

In this section, we first look at the high-frequency limit in both the RPA and MRPA. We find that at finite m_b and large ω_m , there is always a finite difference between the CE-CE and CE-CH Eliashberg anomalous coupling constants. But we find that in the $m_b = 0$ MRPA, the difference is only $\mathcal{O}(\omega_m^{-4})$ at large ω_m . We also derive an explicit formula for the difference in anomalous coupling strength between $l = 0$ CE-CH and $l = 1$ CE-CE, which demonstrates why the MRPA is expected to perform better in the low-frequency limit too. This formula also allows us to propose a possible adjustment to the MRPA, which preserves the correct long-wavelength physics and sum rule behaviour of the MRPA, but guarantees symmetry between the two couplings.

A. A useful formula

In this section, we will take Eq. 40 with the MRPA propagator, and compare CE-CH $l = 0$ and CE-CE $l = 1$. Working through the algebra, we find that

$$\begin{aligned}
 \Delta\lambda_\phi(\omega_m) &= \lambda_\phi^{(l=1),\text{CE-CE}}(\omega_m) - \lambda_\phi^{(l=0),\text{CE-CH}}(\omega_m) = \\
 &= \frac{m^*}{\pi^2 k_F} \int_0^{2k_F} dq \frac{\sqrt{1 - \left(\frac{q}{2k_F}\right)^2} V_{12}(q) [1/\Pi_{11}(q, i\omega_m) - f_1]^2 \times [g(q, i\omega_m)]^2}{\left[\left(1/\Pi_{00}(q, i\omega_m) + f_1 \frac{\omega_m^2}{q^2} - V_{11}(q)\right) (1/\Pi_{11}(q, i\omega_m) - f_1) - \frac{(4\pi)^2}{q^2} \right]^2 - [V_{12}(q) (1/\Pi_{11}(q, i\omega_m) - f_1)]^2}, \\
 g(q, i\omega_m) &= \left(\frac{1}{\Pi_{00}(q, i\omega_m)} + f_1 \frac{\omega_m^2}{q^2} + \frac{2\pi}{m^*} \right)
 \end{aligned} \tag{50}$$

with $f_1 = \frac{m^* - m_b}{n_e}$. We chose units with $k_F = 1$ and $e = 1$, which implies $n_e = \frac{1}{4\pi}$.

B. High-frequency limit

In Eliashberg theory, $q \leq 2k_F$ always, so for $\omega_m \gg \epsilon_F$, we have $q/k_F \ll \omega_m/\epsilon_F$, and some of the results of section IV may be used, namely the forms of Eqs. 41, 42 giving $(1/\Pi_{11} - f_1) \approx 4\pi m_b k_F^2$ and $(1/\Pi_{00} + f_1 \omega_m^2/q^2) \approx -4\pi m_b k_F^2 \omega_m^2/q^2$. Using Eq. 50, we get at $\omega_m \gg \omega_c = 1/m_b$,

$$\Delta\lambda_\phi(\omega_m) = \lambda_\phi^{(l=1),\text{CE-CE}}(\omega_m) - \lambda_\phi^{(l=0),\text{CE-CH}}(\omega_m) = \frac{1}{2\pi^2 k_F \epsilon_F} \int_{q_c}^{2k_F} dq V_{12}(q) \sqrt{1 - \left(\frac{q}{2k_F}\right)^2}. \quad (51)$$

This is divergent, with $\Delta\lambda_\phi(\omega_m) \propto \log q_c$ at small q_c . So there exists an ω_m -independent, $\log q_c$ divergent difference between CE-CE $l = 1$ and CE-CH $l = 0$ when $\omega_m \gg \epsilon_F$. This result is very similar to what we found in section IV, and using Eq. 49 we can see that the most divergent term in the coupling is opposite between the two layers, meaning that for small q_c and large ω_m , $\lambda_\phi^{\text{CE-CE},(l=1)}(\omega_m) > 0$ and $\lambda_\phi^{\text{CE-CH},(l=0)}(\omega_m) < 0$. This is seen for high ω_m in Fig. 3.

Perhaps the more interesting case is MRPA when $m_b = 0$, where all the divergences go away. In order to get a nonzero result, we expand the polarization functions to second lowest order in $\frac{q^2}{\omega_m^2}$, yielding $1/\Pi_{00} \approx -\frac{2\pi}{\epsilon_F} \frac{\omega_m^2}{q^2} \left(1 + 3\epsilon_F^2 \frac{q^2}{\omega_m^2}\right)$ and $1/\Pi_{11} \approx \frac{2\pi}{\epsilon_F} \left(1 - \epsilon_F^2 \frac{q^2}{\omega_m^2}\right)$. Inserting this into Eq. 50 and keeping terms down to $\left(\frac{\epsilon_F}{\omega_m}\right)^4$, we get

$$\Delta\lambda_\phi(\omega_m) \approx \frac{1}{\omega_m^4} \frac{\epsilon_F^3}{32k_F^7} \int_0^{2k_F} dq V_{12}(q) q^6 \sqrt{1 - \left(\frac{q}{2k_F}\right)^2}. \quad (52)$$

This is no longer divergent, and scales as ω_m^{-4} , as opposed to the RPA and finite m_b cases being divergent and scaling as ω_m^0 . This shows that in the high-frequency limit, the MRPA $\Delta\lambda_\phi(\omega_m)$ is much smaller than the RPA counterpart — the MRPA result is much closer to being symmetric between CE-CE and CE-CH pairing than the RPA result is.

C. Low-frequency limit

To find why MRPA would have a lower $\Delta\lambda_\phi(\omega_m)$ at low frequencies, we look at the structure of Eq. 50: the integrand may be written as (prefactor) $\times [g(q, i\omega_m)]^2$. Numerically we observe that the prefactor is strictly positive for a large range of ω_m and q : this can be seen clearly in the large-separation limit, where the second term in the denominator, proportional to V_{12}^2 , becomes very small, and the rest is strictly positive. We thus integrate a positive function, multiplied by $[g(q, i\omega_m)]^2$, which is itself positive. Thus reducing $[g(q, i\omega_m)]^2$ reduces the difference between CE-CE and CE-CH pairing strengths.

Since V_{12} becomes very small for $q \gtrsim 1/d$, in the large- d case at least, most of what contributes to $\Delta\lambda_\phi$ is $[g(q, i\omega_m)]^2$ at small q . We now show that at small q and low frequency, the MRPA has a lower $[g(q, i\omega_m)]^2$. Expanding $g(q, i\omega_m)$ in powers of ω_m at small q , we get

$$\frac{1}{\Pi_{00}(q, i\omega_m)} \approx -\frac{2\pi}{m^*} - \frac{4\pi m^*}{k_F^2} \frac{\omega_m^2}{q^2} + \mathcal{O}(\omega_m^4), \quad (53)$$

$$g(q, i\omega_m) \approx \left(f_1 - \frac{4\pi m^*}{k_F^2}\right) \frac{\omega_m^2}{q^2} + \mathcal{O}(\omega_m^4) = -\frac{4\pi m_b}{k_F^2} \frac{\omega_m^2}{q^2} + \mathcal{O}(\omega_m^4). \quad (54)$$

Importantly, in RPA ($m_b = m^*$) or in finite m_b MRPA, the leading term is $\mathcal{O}(\omega_m^2)$, while for the $m_b = 0$ MRPA the leading term is $\mathcal{O}(\omega_m^4)$. Doing the MRPA cancels the lowest-order term in the Taylor expansion of g , reducing its value at small ω_m and q , which we expect, as discussed, to reduce $\Delta\lambda_\phi(\omega_m)$ at least for low ω_m and large d .

In the last two sections we saw that the MRPA is a step closer to achieving particle-hole symmetry in both low and high frequency limits. As shown in section VII, numeric integration shows it is closer at all ω_m . But there remains a finite difference between $l = 0$ CE-CH and $l = 1$ CE-CE. In the following, we discuss how the MRPA can be adjusted to achieve perfect degeneracy between the two pairing channels.

D. A possible adjustment to the MRPA

A hint on how to achieve full symmetry between CE-CE and CE-CH pairing can be seen in Eq. 50: if we can force $g(q, i\omega_m) = 0$ for all q, ω_m , the pairing would be exactly symmetric. This would amount to replacing the \mathcal{F}_1 of Eq. 19

with an Adjusted MRPA (AMRPA) version

$$\mathcal{F}_{1,\mu\nu}^{\text{AMRPA}}(q, i\omega_m) = \left(1 - \frac{m_b}{m^*} \right) \begin{pmatrix} -\frac{2\pi}{m^*} - \frac{1}{\Pi_{00}(q, i\omega_m)} & 0 \\ 0 & -4\pi k_F^2 m^* + b(q, i\omega_m) \end{pmatrix}_{\mu\nu}, \quad (55)$$

which is then to be used in Eq. 18. If $m_b = 0$, this enforces $g(q, i\omega_m) = 0$. Here the function $b(q, i\omega_m)$ is an arbitrary function, subject to the constraints of causality (no poles in the upper half plane of $b(q, \omega)$), as well as $b(q, \omega) \sim q^n$ for small q with $n \geq 2$ and $b(q, \omega)$ should not grow as fast as ω for large ω . Note that for $b = 0$ the lower right element of the \mathcal{F}_1 matrix matches that of the MRPA. The MRPA \mathcal{F}_1 can be thought of as the AMRPA \mathcal{F}_1 , expanded to the lowest order in q . As such, the two share the same long-wavelength physics, and the AMRPA will satisfy Kohn's theorem. It is also easy to show that the AMRPA satisfies the f-sum rule.

While the AMRPA is designed to give an exact agreement between the coupling strengths of $l = 0$ CE-CH and $l = 1$ CE-CE, it generalises nicely to a general l : within the AMRPA with $m_b = 0$, numeric integration shows that in general l -wave CE-CH is exactly of the same strength as $(l + 1)$ -wave CE-CE, at all frequencies. Since CE-CH is symmetric between l and $-l$, this implies that couplings come in degenerate quadruples: l and $(-l)$ -wave CE-CH, and $(l + 1)$ and $(-l + 1)$ -wave CE-CE. We note that the AMRPA is a correction within *one* layer which brings the different *bilayer* pairing channels to degeneracy.

IX. THE EFFECT OF IMBALANCE

Rüegg, Chaudhary, and Slager[56] have also claimed that CE-CE pairing and CE-CH pairing should be inequivalent because they appear to differ when the layers are imbalanced with the total density remaining $\nu_T = 1$. They argue that for CE-CE pairing the two CE Fermi seas would become mismatched in size when electrons are transferred from one layer to another, whereas for CE-CH pairing the two Fermi seas remain the same size. This statement is incorrect, as it does not account for the change in the Chern-Simons magnetic field that occurs when density is changed. As mentioned by Wagner et al.[51] (Supplementary material), both cases are equally suited to pairing in the imbalanced case. For completeness we reiterate this argument here.

We keep the total filling $\nu_T = 1$ fixed, but move some density from one layer to the other so that we have $\nu = \nu_1 + \nu_2$ with $\nu_1 \neq \nu_2$. For simplicity, let us consider the case where $\nu_1 = p/(2p + 1)$, potentially with p large. This single layer can be described as p filled CE Landau levels. The opposite layer has filling $\nu_2 = (p + 1)/(2p + 1)$ but this can also be viewed as a filling of $1 - \nu_2 = p/(2p + 1)$ of holes, and can be described as p filled CH Landau levels. To build a CE-CH pairing we simply pair the states of the n^{th} CE Landau level of the first layer with those of the n^{th} CH Landau level of the second layer[51]. However, the second layer can also be thought of as $p + 1$ filled Landau levels of CEs in a negative magnetic field. While the description of the p filled Landau levels of CHs is different from that of $p + 1$ filled Landau levels of CEs, these two descriptions make almost identical predictions[12, 14, 63]. In particular, the number of states per Landau level is the same and the low energy excitations are in one-to-one correspondence. To build a CE-CE pairing in this picture, one pairs the states of the $(p + 1)$ th Landau level of CEs in the second layer with the states of the p th Landau level of CEs in the first layer. As we show below, this is in fact necessary in order to obtain an $l = 1$ BCS state. This allows a perfectly good BCS paired state, except that the lowest Landau level of CEs in the second layer remains unpaired. However, since this Landau level is buried far below the Fermi surface, it can be considered to be completely filled without any energetic penalty.

A. Pairing symmetry in the imbalanced case

In this section, we prove generally that when Landau levels n and $n + l$ are BCS-paired in the imbalanced $\nu_T = 1$ case, the resulting pair wave function always has l -wave symmetry, both for CE-CE and CE-CH pairing. We take $\nu_\uparrow = \frac{p+1}{2p+1}$, $\nu_\downarrow = \frac{p}{2p+1}$. If the physical magnetic field is B_0 , the effective fields seen are then exactly opposite between the two layers, defining $B = \frac{1}{2p+1}B_0$, $B_\uparrow = -\frac{1}{2p+1}B_0 = -B$ and $B_\downarrow = \frac{1}{2p+1}B_0 = B$. From now on we work in units where the effective magnetic length, $l_B = \sqrt{\frac{\hbar}{eB}} = 1$. Then, in a planar geometry, the single-particle wavefunctions are in the Landau gauge,

$$\Psi_{n,k}^\uparrow(\mathbf{r}) = e^{iky} \phi_n(x + k) \quad (56)$$

$$\Psi_{n,k}^\downarrow(\mathbf{r}) = e^{iky} \phi_n(x - k) \quad (57)$$

$$\phi_n(x) = \frac{1}{\pi^{1/4} \sqrt{2^n n!}} e^{-x^2/2} H_n(x), \quad (58)$$

with $H_n(x)$ the n -th order physicist's Hermite polynomial.

Case 1: CE-CE pairing

BCS pairing occurs between an electron of momentum k in LL $n+l$ of one layer and an electron of momentum $-k$ in LL n in the other, for all n . So the BCS pair function may be constructed as

$$g_l(\mathbf{r}^\uparrow, \mathbf{r}^\downarrow) = \sum_{n=0}^{p-1} g_n f_l^n(\mathbf{r}^\uparrow, \mathbf{r}^\downarrow), \quad (59)$$

$$f_l^n(\mathbf{r}^\uparrow, \mathbf{r}^\downarrow) = \int dk \Psi_{n+l,k}^\uparrow(\mathbf{r}^\uparrow) \Psi_{n,-k}^\downarrow(\mathbf{r}^\downarrow). \quad (60)$$

Here, g_n are constants to be determined from energetic considerations. The function f_l^n is the main object of interest and using Eqs. 56, 57 we may write it as

$$f_l^n(\mathbf{r}^\uparrow, \mathbf{r}^\downarrow) = \int dk e^{ik(y^\uparrow - y^\downarrow)} \phi_{n+l}(x^\uparrow + k) \phi_n(x^\downarrow + k) \quad (61)$$

Case 2: CE-CH pairing

Here, both layers are less than half-full of the carriers, so the wavefunction Eq 57 is to be used for both. Now we pair a hole of momentum k in one layer to an electron of momentum k in the other. Taking the hole to be in the up layer, making the replacement $k \rightarrow -k$ in Eq. 57 and remembering that the hole wavefunction must be complex conjugated we get, since ϕ_n is real,

$$g_l(\mathbf{r}^\uparrow, \mathbf{r}^\downarrow) = \sum_{n=0}^p g_n f_l^n(\mathbf{r}^\uparrow, \mathbf{r}^\downarrow), \quad (62)$$

$$f_l^n(\mathbf{r}^\uparrow, \mathbf{r}^\downarrow) = \int dk e^{ik(y^\uparrow - y^\downarrow)} \phi_{n+l}(x^\uparrow + k) \phi_n(x^\downarrow + k). \quad (63)$$

This exactly matches the expression Eqs. 59, 61, for CE-CE, so both may be treated simultaneously from now on.

To evaluate f_l^n explicitly, we define $\mathbf{R} = \frac{1}{2}(\mathbf{r}^\uparrow + \mathbf{r}^\downarrow)$ and $\mathbf{r} = \frac{1}{2}(\mathbf{r}^\uparrow - \mathbf{r}^\downarrow)$. Using these in Eq. 61, and putting $q = k - X + x/2$, we get

$$f_l^n(\mathbf{R}, \mathbf{r}) = e^{i(\frac{x}{2} - X)y} \int dq e^{iqy} \phi_{n+l}(x+q) \phi_n(q) \quad (64)$$

Using Eq. 58, we can get

$$f_l^n(\mathbf{R}, \mathbf{r}) = C_l^n e^{i(\frac{x}{2} - X)y} \int dq e^{iqy} e^{-\frac{(x+q)^2}{2} - \frac{q^2}{2}} H_{n+l}(x+q) H_n(q) \quad (65)$$

$$f_l^n(\mathbf{R}, \mathbf{r}) = C_l^n e^{-iXy} e^{-\frac{1}{4}(x^2 + y^2)} \int dk e^{-k^2} H_{n+l}(k + \frac{x+iy}{2}) H_n(k - \frac{x-iy}{2}) \quad (66)$$

Here, $C_l^n = \frac{1}{\sqrt{\pi 2^{2n+l} n! (n+l)!}}$ is a constant. Going between Eq. 65 and Eq. 66, we re-wrote the exponential as $iqy - \frac{(x+q)^2}{2} - \frac{q^2}{2} = -(q + \frac{x-iy}{2})^2 - \frac{1}{4}(x^2 + y^2 + 2ixy)$. We then defined $k = q + \frac{x-iy}{2}$. The H_n are just polynomials and may be recovered exactly by Taylor expansion: letting $H_n^{(s)}(x) = \frac{d^s}{dx^s} H_n(x)$ and defining $z = (x+iy)/2$, we may write exactly

$$H_{n+l}(k+z) = \sum_{s=0}^{n+l} H_{n+l}^{(s)}(k) \frac{z^s}{s!} \quad (67)$$

$$H_n(k-\bar{z}) = \sum_{t=0}^n H_n^{(t)}(k) \frac{(-\bar{z})^t}{t!}. \quad (68)$$

Noting the Hermite polynomial identities

$$H_n^{(s)}(x) = 2^s s! \binom{n}{s} H_{n-s}(x), \quad (69)$$

$$\int dx H_m(x) H_n(x) e^{-x^2} = \sqrt{\pi} 2^n n! \delta_{n,m}, \quad (70)$$

we use Eq. 69 in Eq. 66 to get

$$f_l^n(\mathbf{R}, \mathbf{r}) = C_l^n e^{-iXy} e^{-\frac{1}{4}(x^2+y^2)} \sum_{t=0}^n \sum_{s=0}^{n+l} \binom{n+l}{s} \binom{n}{t} (x+iy)^s (x-iy)^t \int dk H_{n-t}(k) H_{n+l-s}(k) e^{-k^2} \quad (71)$$

$$f_l^n(\mathbf{R}, \mathbf{r}) = e^{-iXy} (x+iy)^l F_l^n(|\mathbf{r}|^2) \quad (72)$$

$$F_l^n(|\mathbf{r}|^2) = C_l^n e^{-\frac{1}{4}|\mathbf{r}|^2} \sum_{t=0}^n \binom{n+l}{t+l} \binom{n}{t} (-|\mathbf{r}|^2)^t \sqrt{\pi} 2^{n-t} (n-t)!$$

To get to the second line, we used Eq. 70 and assumed $l \geq 0$.

The prefactor e^{-iXy} in Eq. 72 is a center of mass momentum in the X direction depending on the separation in the y direction. This stems from the non-commutativity of x and y coordinates in a magnetic field, and is reminiscent of the physics of excitons in a magnetic field (see for example Ref. [64]).

The remainder of Eq. 72 has the form $(x+iy)^l F_l^n(|\mathbf{r}|^2)$ for all \mathbf{r} , characteristic of an l -wave state. We note that $F_l^n(|\mathbf{r}|^2)$ is just a polynomial of order n in $|\mathbf{r}|^2$, multiplied by a Gaussian factor. Of course the final pair wavefunction is $g_l(\mathbf{r})$, where all the angular dependencies factor out, and we get from Eqs. 59,72

$$g_l(\mathbf{R}, \mathbf{r}) = (x+iy)^l e^{-iXy} G_l(|\mathbf{r}|) \quad (73)$$

$$G_l(|\mathbf{r}|) = \sum_{n=0}^{p-1} g_n F_l^n(|\mathbf{r}|^2) = e^{-\frac{1}{4}|\mathbf{r}|^2} \sum_{n=0}^{p-1} g_n C_l^n \sum_{t=0}^n \binom{n+l}{t+l} \binom{n}{t} (-|\mathbf{r}|^2)^t \sqrt{\pi} 2^{n-t} (n-t)!,$$

clearly showing an l -wave pair wavefunction for $l \geq 0$. We note that $G_l(|\mathbf{r}|)$ is just a polynomial of order $p-1$ in $|\mathbf{r}|^2$, multiplied by the Gaussian factor $e^{-\frac{1}{4}|\mathbf{r}|^2}$. This result can be trivially generalised to $l < 0$: there, we get $g_l(\mathbf{R}, \mathbf{r}) = e^{-iXy} (x-iy)^{|l|} G_l(|\mathbf{r}|^2)$, which gives a $-|l| = l$ -wave state, as expected.

To re-iterate our argument, in the case of CE-CH pairing, there are p filled Landau levels in each layer: we may pair levels n and n for $0 \leq n \leq p-1$, giving us an $l = 0$ BCS state. In the case of CE-CE pairing, there are $p+1$ LLs in the upper layer and p in the lower. We pair level $n+1$ in the upper layer to level n in the lower layer for $0 \leq n \leq p-1$. This results in an $l = 1$ BCS state, and only the LLL of the upper layer remains unpaired. This level is far below the Fermi surface, and as such the fact that it remains unpaired should not significantly impact the pairing strength.